MASTER OF SCIENCE

Analysis of the composition and regulation of the SLX4 complex

Satriano, Letizia

Award date:
2014

MASTER OF SCIENCE

Analysis of the composition and regulation of the SLX4 complex

Letizia Satriano

2014

University of Dundee

Analysis of the composition and regulation of the SLX4 complex

By

Letizia Satriano

A thesis submitted for the degree of Master of Science, University of Dundee

March 2014

Table of contents

List of figures

List of tables

Amino acid code

Amino acid	Three letters code symbol	One letter
Alanine	Ala	A
Arginine	Arg	R
Asparagine	Asn	N
Aspartic acid	Asp	D
Cysteine	Cys	C
Glutamic acid	Glu	E
Glutamine	Gln	Q
Glycine	Gly	G
Histidine	His	H
Isoleucine	Iso	I
Leucine	Leu	L
Lysine	Lys	K
Methionine	Met	M
Phenylalanine	Phe	F
Proline	Pro	P
Serine	Ser	S
Threonine	Thr	T
Tryptophan	Trp	W
Tyrosine	Tyr	Y
Valine	Val	V

Abbreviations

AML	Acute Myeloid Leukemia
Amp	Ampicillin
ATM	Ataxia Telangiectasia Mutated
ATR	ATM and Rad3 related
BS	Bloom's Syndrome
BSA	Bovine Serum Albumine
C-terminal	Carboxy-terminal
CDK	Cyclin Dependent Kinase
DMSO	Dimethylsulphoxide
DNA	Deoxyribonucleic acid
DSB	Double Strand Break
DSTT	Division of Signal Transduction Therapy
ECL	Enhanced Chemiluminescence
EDTA	EthyleneDiamide Tetraacetic Acid
EGTA	EthylenGlycol bis (2-aminoethyether)- N'N'tetraacetic Acid
ERCC4	Excision Repair Cross Complementation group 4
FA	Fanconi Anemia
FACS	Fluorescence Activated Cell Sorting
HECT	Homologous to the E6AP Carboxyl Terminus
HR	Homologous Recombination
HPLC	High Pressure Liquid Chromatography
HU	Hydroxyurea
ICL	Interstrand Crosslinks
IP	Immunoprecipitation
kDa	KiloDalton
LB	Luria Bertani medium
LDS	Lithium Dodecyl Sulphate
M	Molar
MALDI-TOF	Matrix-assisted laser desorption/ionization
MDS	Myelodysplastic Syndrome
MMC	Mitomycin C
MMR	Mismatch Repair
MRC PPU	Medical Research Council Protein
MS	Mass Spectrometry
NER	Nucleotide Excision Repair
PBS	Phosphate Buffer Saline
PCR	Polymerase Chain Reaction
PI 3-kinase	Phosphatidylinositole 3-kinase
Rpm	revolutions per minute

RING	Really Interesting New Gene
ROS	Reactive Oxygen Species
SSA	Single Strand Annealing
TAE	Tis-Acetate EDTA
TBS	Tris-buffer Saline
TLS	Translesion Synthesis
XP	Xeroderma Pigmentosum

SUMMARY

The human SLX4 is a scaffold protein that coordinates multiple partners and it is involved in interstrand crosslinks repair, as well as in the resolution of Holliday junctions.

In this thesis I performed for the first time a phospho-mapping analysis of the endogenous SLX4, immunoprecipitated from untreated or MMC-treated cells. This experiment led to the identification of ATM/ATR phospho-sites, as well as sites that could be targeted by proline-directed kinases. Although the meaning of the SLX4 phosphorylation is still unclear, it could be possible that this modification affects the binding between SLX4 and some of its partners. In this regard, I found that SLX4-MUS81 interaction is dynamic. The amount of MUS81 in SLX4 immunoprecipitates was reduced after exposing cells to genotoxins, such as MMC, CPT, and HU. Moreover cell-cycle experiments using counterflow centrifugal elutriation showed that the binding between the two proteins increases in S/G2 phase.

In the second section, mass fingerprinting analysis of endogenous SLX4 immunoprecipitates, showed that the complex binds also to two E3 ligases: the E3 RING SCF^{FBXO11} complex and the HECT E3 UBR5 and these interactions were confirmed by immunoprecipitation. SCF^{FBXO11} and UBR5 target their substrates to protein degradation, but preliminary experiments showed that the interactions did not affect the overall quantity of SLX4 or the binding with its nucleases.

Finally I showed that the endogenous SLX4 interacts with the mismatch repair (MMR) complex MSH2-MSH3 by immunoprecipitation. Moreover, from yeast two hybrid assay it appeared that MSH2 directly binds to SLX4 and the binding involves the N-terminal region of SLX4. If this direct binding will be confirmed, I will investigate whether the MSH2-MSH3 complex plays a role in ICL repair or in Holliday junctions resolution pathway.

1 INTRODUCTION

1.1 The DNA damage response

Genome integrity is constantly threatened by endogenous and exogenous factors that cause DNA damage. DNA damage needs to be repaired quickly in order to avoid errors that could lead to genome instability and the development of diseases such as cancer. Endogenous factors that cause DNA damage include byproducts of oxidative metabolism, such as reactive oxygen species (ROS) that can induce oxidation of DNA bases, as well as errors arising from base misincorporation during replication. Exogenous factors include UV light which causes pyrimidine dimers that can impede the progression of DNA replication and transcription machineries, and ionizing radiation which can induce DNA single-strand and double-strand breaks. Many drugs used in chemotherapy of cancer act by inducing DNA damage and these include hydroxyurea (HU) which blocks the replication fork by inhibiting the production of dNTPs, and mitomycin-C (MMC) and cisplatin which can covalently crosslink bases on the same (intrastrand) or opposite (interstrand crosslinks) DNA filaments.

1.2 Interstrand DNA crosslinks

Interstrand DNA crosslinks (ICLs) are particularly toxic lesions, because they prevent the two DNA strands from separating, thereby perturbing DNA replication and transcription. In fact, it has been estimated that as few as twenty interstrand crosslinks in the mammalian genome can be lethal to cells that lack the ability to remove the crosslink (Lawley et al. 1996; Murnane et al. 1981). ICLs are caused by both endogenous and exogenous factors. Among the endogenous agents are unsaturated

aldehydes and nitric oxide (Kirchner et al. 1992). Unsaturated aldehydes are derived from lipid peroxidation and the metabolism of dietary components such as coffee and alcohol (Stone et al. 2008; Huang et al. 2010a; Garaycoechea et al. 2012); nitric oxide can also be linked to diet as it is a by-product of nitrates used to preserve meat, but it is also a signaling molecule important for vasoregulation (Kirchner et al. 1992; Guainazzi et al. 2010). Nitrogen mustards, mitomycin C, psoralen, and platinum compounds like cisplatin are exogenous agents that produce a mixture of monoadducts and ICLs and they are commonly used in cancer therapy to kill tumor cells (Lawley et al. 1996; McHugh et al. 2001). However, these treatments also induce ICLs in normal cells (McHugh et al. 2001), and it has been shown an increase in the incidence of acute myeloid leukemia (AML) in patients treated with ICL-inducing agents (Tucker et al. 1988; Travis et al. 1999). Regardless of the source of ICLs, cells have developed mechanisms to detect and repair these lesions.

1.2.1 Repair of interstrand crosslinks

The first cohesive model for ICL repair in *Escherichia coli* was proposed by Ronald Cole in 1973. Using cells containing psoralen-induced ICLs, he proposed a repair mechanism that involved a partial excision of the crosslink, followed by strand exchanges between homologous filaments (Cole, 1973). In lower eukaryotes, studies performed on *S. cerevisiae* showed the involvement of three distinct pathways: nucleotide excision repair (NER), post-replication repair and homologous recombination (HR) (Jachymczyk et al., 1981; Grossman et al., 2001). In mammalian systems the situation appears to be more complicated, but progress in understanding the molecular mechanisms of ICL repair have been greatly aided by studying the human genetic disorder Fanconi

Anemia (FA). This is a rare inherited syndrome, with an incidence of 1 to 5 per 10^6 births, with clinical features that are very heterogeneous in nature. Patients can present with skeletal abnormalities such as hypoplasia of the thumbs and radial hypoplasia, skin pigmentation, developmental disorders and cancer such as squamous cell carcinoma of the head or neck and hepatocellular carcinoma (Tischkowitz et al., 2003; Fanconi, 1967; D'andrea et al., 2010). During childhood, most FA patients manifest hematological abnormalities: aplastic anemia, myelodysplastic syndrome (MDS) and acute myeloid leukemia (AML) (Tischkowitz et al., 2003). Given the heterogeneity of the syndrome, a diagnosis based only on clinical features is difficult. However in 1988 Auerbach and colleagues developed a test for FA based on the hypersensitivity of FA lymphocytes to crosslinking drugs. Agents like mitomycin C or diepoxybutane induce chromosomal abnormalities in FA cells such as radial chromosomes and chromosome breakage (Auerbach et al., 1988). This observation led to the assumption that the FA syndrome is linked with the interstrand crosslink repair pathway.

ICL repair in mammalian is still poorly understood but it is clear that it is a complicated process that involves the cooperation of multiple pathways: the FA pathway, homologous recombination (HR), translesion synthesis (TLS) and nucleotide excision repair (NER) (McCabe et al., 2009; D'andrea et al., 2012). ICL repair can take place in G1 phase of the cell cycle (Wang et al., 2001; Muniandy et al., 2009) but it is thought that the predominant mode of repair occurs during the S phase, induced by the collision of one of more replication forks with the ICL (Akkari et al., 2001; Rothfuss et al., 2004). At present, there are three major models that have been put forward to account for replication-coupled ICL repair. In the first, repair initiates when a single

replication fork stalls at an ICL lesion, and DNA replication resumes when the repair is completed by homologous recombination (Niedernhofer et al., 2005). The second model is somewhat similar to the first but the stalled replisome traverses the ICL with the help of FANCM, and the repair of the ICL itself is post-replicative (Huang et al. 2013). In the third model, two replication forks stall on an ICL and as in the second model, the repair is post-replicative (Raschle et al., 2008) (**Fig.1**).

1.2.1.1 Models to explain ICL repair

In the first model, the collision of the replication fork with the ICL recruits various FA proteins, possibly starting with FANCM. This protein has a translocase activity, which might remodel the fork, leading to recruitment of the FA core complex in collaboration with FAAP20 and RNF8 (Gari, Decaillet et al. 2008; Yan, Guo et al. 2012). The FA core complex includes nine polypeptides that together comprise an E3 ubiquitin ligase which ubiquitinates two paralogous FA proteins, FANCD2 and FANCI (Alpi and Patel 2009). As discussed later, ubiquitination of FANCD2 signals fork stalling and helps to initiate ICL repair. An early step of ICL repair is “unhooking” which involves dual incisions on either side of the ICL. This results in a “flipping out” of the ICL and fork breakage leading to generation of a one-ended double strand break (Fig.1, first model). The gap created by unhooking is filled in by TLS past the damaged oligonucleotide, which is subsequently removed by a NER mediated cleavage. Finally HR restores the replication fork so that DNA replication can resume (Niedernhofer, Lalai et al. 2005). In the second model, repair of the ICL is uncoupled from DNA replication. DNA fiber analysis shows that the replication machinery can traverse an ICL lesion, in a manner that requires FANCM. When a replication fork stalls by an ICL, FANCM might translocate the all complex past the ICL onto the non-replicated

strands (**Fig.1**, second model). This would allow cells to restart the replication and to repair the ICL lesion by postreplication pathways (Huang, Liu et al. 2013).

The third model, proposed by Räschle and colleagues, comes from experiments carried out in cell-free extracts of *Xenopus* that monitor the repair of a plasmid bearing a site-specific ICL. The plasmid is small, with a single origin of replication and both forks emanating from this origin encounter the ICL. This system has been very useful in visualizing steps involved in ICL repair, but by necessity it invokes two forks hitting the ICL. In this model, the two replication forks encountering the ICL stall around 20 nucleotides before the crosslink (**Fig.1**, third model). Prior to the uncoupling step, a TLS polymerase extends the nascent strand within one nucleotide from the ICL and only later on the ICL incision step takes place. After that, a nucleotide is inserted across from the damaged template base and then the leading strand is extended beyond the ICL by a translesion DNA polymerase. Finally the lesion is excised and HR restores the replication fork. As mentioned before, the model was proposed based on experiments performed using a cell-free system based on *Xenopus* egg extracts using plasmids containing single nitrogen mustard-like or cisplatin ICL. Although this system is useful for studying a single ICL lesion, it is unclear whether it would accurately reflect ICL repair *in vivo* (Raschle et al., 2008).

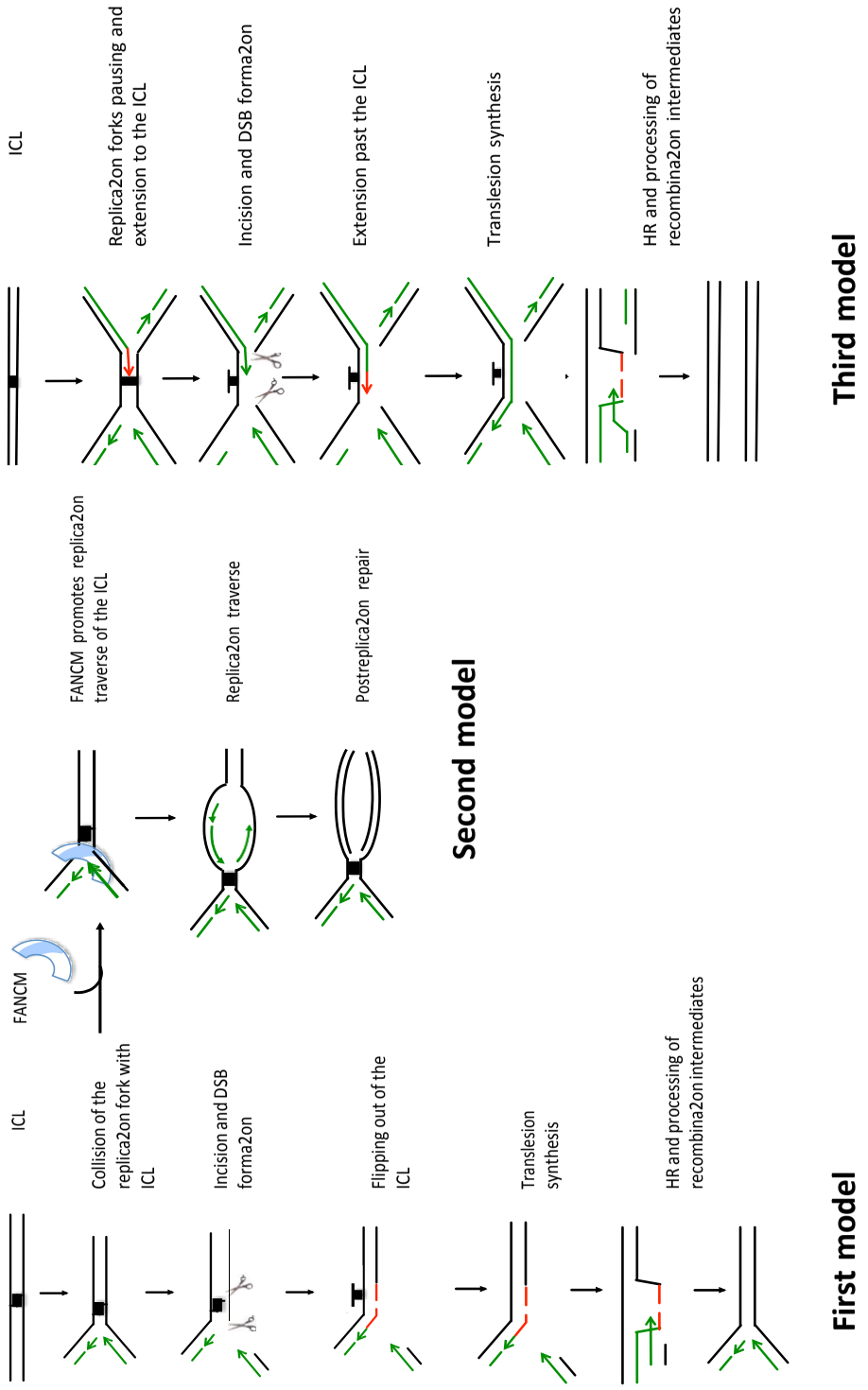

Figure 1: Schematic view of the three possible models for the repair of ICLs.

1.3 FA and FA-associated proteins

As mentioned before, FA syndrome is linked with the ICL repair pathway, and many genes essential to the repair of ICLs were discovered to be mutated in FA patients. Currently there are 16 FANC complementation groups: *FANCA, FANCB, FANCC, FANCD1, FANCD2, FANCE, FANCF, FANCG, FANCI, FANCJ, FANCL, FANCM, FANCN, FANCO, FANCP* and *FANCQ.* Some of the proteins are required for sensing the damage and others are directly implicated in the repair of the ICL lesion (**Table 1**).

FA protein	Biochemical activity
FANCA	Core complex member required for the ID ubiquitination
FANCB	Core complex member required for the ID ubiquitination
FANCC	Core complex member required for the ID ubiquitination
FANCD1/BRCA2	HR mediator
FANCD2	Member of the ID, ubiquitinated after DNA damage
FANCE	Core complex member required for the ID ubiquitination
FANCF	Core complex member required for the ID ubiquitination
FANCG	Core complex member required for the ID ubiquitination
FANCI	Member of the ID, ubiquitinated after DNA damage
FANCJ/BRIP1	Helicase
FANCL	E3 ligase of the core complex
FANCM	Helicase that recruites the core complex to the chromatin
FANCN/PALB2	FANCD1 interactor
FANCO/RAD51C	HR mediator
FANCP/SLX4	HR mediator and FANCQ interactor
FANCQ/XPF	endonuclease

Table 1: The sixteen complementation groups of FA and their related activity in the FA pathway.

The FANCM subunit initiates the pathway possibly by binding to DNA discontinuities at the stalled fork; exactly how FANCM is recruited is unclear but it appears to involve other proteins (Ciccia et al. 2007; Yan et al. 2010; Singh et al. 2010). FANCM is a

member of the XPF family of endonucleases together with XPF-ERCC1, MUS81-EME1, and MUS81-EME2. In eukaryotes all the members of this family exist as heterodimers consisting of an active-nuclease subunit (XPF, MUS81) and a non-catalytic subunit (ERCC1, EME1, EME2). The catalytic form presents a core Excision Repair Cross Complementation group 4 (ERCC4) endonuclease domain and a Helix-hairpin-Helix (HhH) domain. The non-catalytic counterpart retains the ERCC4 module, but lacks key residues for the endonuclease activity (Ciccia et al. 2008). Although FANCM is an XPF-like protein, it lacks the endonuclease activity, but it binds to branched DNA structures *in vitro* and exhibits an ATP-dependent translocase activity. In 2007 Steve West's lab discovered FAAP24, the ERCC1-like partner of FANCM (Ciccia et al. 2007). The binding of FAAP24 to FANCM stabilizes the association of FANCM with single stranded DNA and is thought to lead to the recruitment of the FA core complex to chromatin in an S-phase dependent manner (Ciccia et al. 2007; Kim et al. 2008). Moreover, the binding of FANCM to the chromatin is assisted by two histone-fold containing proteins, MHF1 and MHF2 that stimulates replication fork remodelling (Yan et al. 2010; Singh et al. 2010).

The correct assembly of the core complex is crucial for proper downstream signaling such as the monoubiquitination of the FANCD2/FANCI complex (also called the "ID" complex). The ubiquitination of FANCD2 by the FA core complex is catalyzed by the E3 RING-type ubiquitin ligase FANCL (Alpi et al. 2009). FANCL belongs to the FA core complex together with seven other FANC proteins (see **Table 1**), but FANCL seems to be the only component with intrinsic ligase activity (Alpi et al. 2009; Meetei et al. 2003). The monoubiquitination of FANCD2 by FANCL is required for the targeting and accumulation of FANCD2 in nuclear foci at sites of DNA damage (Garcia et al. 2001; Taniguchi et al. 2002). Ubiquitination of FANCD2 was also found to be required for the

unhooking, translesion synthesis and homologous recombination steps of ICL repair, at least in the *Xenopus* cell-free system (Knipscheer et al. 2009; Räschle et al. 2008).

The encounter of an ICL by the replication fork, leads to the recruitment of nucleases. FAN1, which displays both a 5'-3' exonuclease and 5' flap endonuclease activity, is recruited to the stalled fork via its interaction with the monoubiquitinated FANCD2 (MacKay et al. 2010). This binding requires the UBZ4-type ubiquitin-binding zinc finger domain present on FAN1 (Liu et al. 2010; Smogorzewska et al. 2010; Kratz et al. 2010; MacKay et al. 2010).

The role of FAN1 in ICL repair is not clearly understood: although FAN1 is a nuclease and is recruited by FANCD2, it is probably not required for ICL unhooking. Several laboratories proposed that the initiation of the unhooking might be mediated by the structure-specific nuclease MUS81-EME1 (Hanada et al. 2006; Hanada et al. 2007), followed by a second incision by the heterodimeric nuclease XPF-ERCC1 (Bergstralh et al. 2008; Bhagwat et al. 2009). However, Wang and colleagues found evidence of a third nuclease, SNM1A that participates in the unhooking event (Wang et al. 2011). In this model, the first incision is mediated by XPF-ERCC1, followed by an SNM1A exonucleolytic digestion of the cross-linked oligonucleotide. In this context, MUS81-EME1 requirement could be limited to a backup activity, in case of a failure in the XPF-SNM1A pathway.

The incision of the ICL leads to the formation of a DSB in the lagging strand and an unhooked ICL on the leading strand and TLS polymerases, like REV1 and Pol ζ extend

across the adduct (Sharma and Canman 2012). Finally homologous recombination completes the reaction (**Fig.1**).

1.4 The mammalian SLX4 complex

SLX4 is a scaffold protein that coordinates a multi-protein complex involved in repair of DNA interstrand crosslinks. SLX4 has no obvious catalytic motifs but it is contains several modular domains (**Fig. 2**). At the N-terminus there are two UBZ4 domains (ubiquitin-binding zinc finger domain 4), followed by an MLR domain (MEI9-Interaction-Like Region), a BTB/POZ domain (Broad-Complex, Tramtrack and Brick a brax/Poxvirus and Zinc finger), a SAP domain (SAF-A/B, Acinus and PIAS), and at the C-terminal end there is an HtH motif (Helix turn Helix). SLX4 interacts with three structure-selective endonucleases: XPF-ERCC1, MUS81-EME1 and SLX1, which bind to the MLR, SAP and HtH domains respectively (Fekairi et al., 2009; Kim et al., 2013; Svendsen et al., 2009; Castor et al. 2013). SLX4 also associates with the mismatch repair complex (MSH2-MSH3), shelterin factors TRF2-RAP1, the nuclease hSNM1B/Apollo (Salewsky et al., 2012), the protein kinase PLK1 and an uncharacterized protein, C20ORF94 (Svendsen et al., 2009) (**Fig.2**).

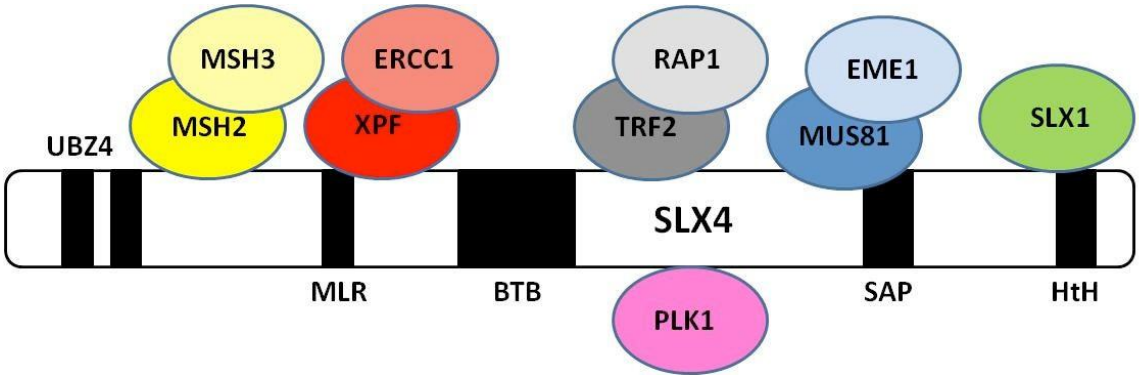

Figure 2: SLX4 complex showing all the known SLX4 domains and interactors.
The positions of Apollo and C24ORF94 on the scaffold are still unknown.

1.5 SLX4 complex in ICL repair

The importance of SLX4 in ICL repair was underlined by two main observations. First of all cells depleted of SLX4 are sensitive to ICL drugs, like camptothecin and MMC (Svendsen et al., 2009; Muñoz et al., 2009), secondly and most importantly it has been discovered that bi-allelic mutations in SLX4 cause Fanconi Anemia (Stoepker et al., 2011; Kim et al., 2011; Kim et al., 2013). Hence, SLX4 was characterized as a recent addition to the FA group of proteins and is sometimes referred to as FANCP on this basis.

A range of SLX4 mutations have been identified in FA (Stoepker et al., 2011; Kim et al., 2011). In some patients, cells have been found to express very low concentrations of a truncated form of SLX4, which retained all known modules, and which was capable of interacting with XPF-ERCC1, MUS81-EME1 and SLX1 (Stoepker et al., 2011; Kim et al., 2011). In three siblings from a different family, the level of SLX4 expression was not altered but the protein carried a small deletion that removed a fragment containing part of UBZ1 and all UBZ2 domain (Stoepker et al., 2011; Kim et al., 2011). These data indicate the SLX4 UBZ domains are required for ICL repair. Although the precise role of the UBZ domains still need to be unraveled, analysis from the Rouse lab found that the UBZ1 binds to K63-linked polyubiquitin chains and it is the key domain required for the recruitment of SLX4 at sites of DNA damage. However the recruitment seems to be independent of FANCD2 (JR, personal communication), despite reports to the contrary for SLX4 in chicken DT-40 cells (Yamamoto, Kobayashi et al. 2011).

It is not clear at what stage of ICL repair SLX4 acts. In cells lacking, or depleted of SLX4, FANCD2 is ubiquitinated normally and double strand breaks are induced. However, a

subset of these breaks persists indefinitely and cells die (Munoz et al., 2009). A role for unhooking for SLX4, for example by COMET assay has not been reported, but the data above could be interpreted to mean that SLX4 is required for the completion of HR at the final stages of ICL repair. This is especially likely given that the SLX4 complex has been strongly implicated in late-stage DNA intermediate processing in HR outside of ICL repair, as discussed below.

1.6 SLX4 complex in resolution of HJs

Homologous recombination (HR) is a conserved mechanism for repairing DNA double-strand breaks during meiosis and unscheduled DNA breaks. Perhaps the most important function for HR is the repair of DSBs produced by stalled or collapsed replication forks. Holliday junctions (HJs) are four way DNA intermediates that arise during homologous recombination, points at which two chromatids become topologically linked. These structures must be removed, as their persistence through mitosis would prevent chromosome segregation. Two major pathways have been described for the removal of HJs in mitotic mammalian cells: dissolution and resolution.

Dissolution of double HJs is mediated by the BTR complex that comprises the RecQ-type helicase BLM, which forms a four subunit complex together with DNA topoisomerase III, RMI1 and RMI2 (Wu et al., 2003). This mode of HJ removal involves only non-crossover products (**Fig.3**) (Wu et al., 2003). It is probably for this reason that dissolution is the dominant HJ removal pathway in mitotic cells, to avoid loss-of-heterozygosity that would compromise fitness. In this light, mutations in BLM cause Bloom's syndrome (BS), a recessive disorder characterized by cancer predisposition

(Mohaghegh and Hickson 2001). Cells from BS patients show increased loss of heterozygosity, and a high degree of sister chromatin exchange (SCE) probably caused by increased crossover frequency (Chaganti, Schonberg et al. 1974; Wu et al. 2003, 2006).

The resolution of HJs that escape dissolution is mediated by specialized endonucleases that cleave DNA intermediates, yielding to either crossover or non-crossover products. In human cells these endonucleases are MUS1-EME1 (Chen et al., 2001; Ciccia et al., 2003), SLX1 (Fekairi et al., 2009; Munoz et al., 2009; Svendsen et al., 2009), and GEN1 (Ip et al., 2008; Matos et al., 2011) (**Fig.3**). These enzymes have different *in vitro* substrates specificities. GEN1 is a canonical HJ resolvase that cleaves 4-way DNA junctions symmetrically, and among the three, it is the only nuclease that does not bind to the SLX4 scaffold. The second nuclease, MUS81-EME1 belongs to the ERCC4 family of endonucleases and as for XPF-ERCC1, it is composed of a catalytic subunit (MUS81) and a non-catalytic partner (EME1) (Ciccia et al., 2003). The complex has a preference for 3'-flaps, replication forks and nicked HJs, but only weakly cleaves intact HJs (Ciccia et al., 2003). SLX1 is the third enonuclease involved in the resolution pathway, it belongs to a family of UvrC-type endonucleases and it consists of a URI nucleases domain and a PHD-type Zinc finger motif (Aravind et al., 2001). In human cells it is stable only in complex with SLX4, and it cleave HJs, replication forks, and 3'-5' flaps (Fekairi et al., 2009; Munoz et al., 2009; Svendsen et al., 2009).

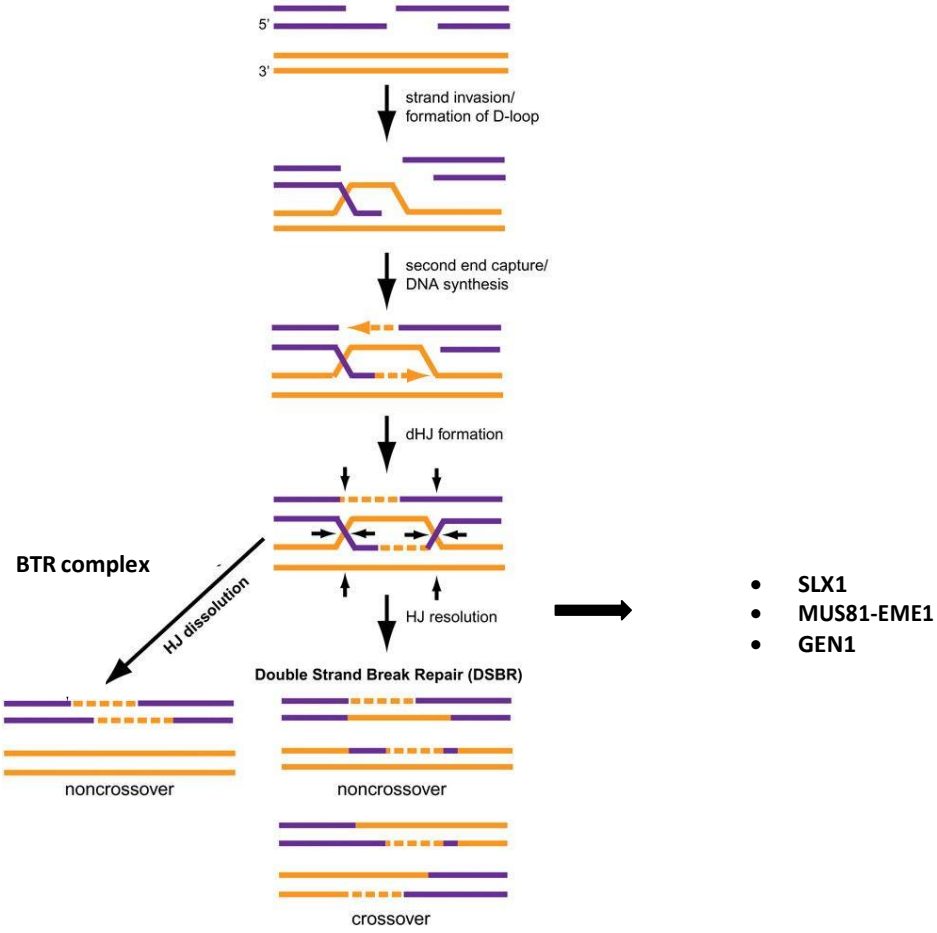

Figure 3: Repair of DSBs by either the recombinogenic or the non-recombinogenic pathways. (Adapted from Svedsen and Harper, 2010).

In vitro and *in vivo* experiments demonstrated that the SLX4 complex plays a role in the resolution of HJs in human cells and this activity resides in its C-terminal region where MUS81 and SLX1 bind (Svendsen et al., 2009). The spatial proximity of MUS81 and SLX1 on SLX4 coordinates the combined and temporally regulated cleavage of HJs by the two nucleases. In the current model, SLX1 acts first by nicking the HJ, then the nicked intermediate is acted upon by MUS81 to produce linear duplexes (Wyatt et al., 2013; Castor et al., 2013). In 2013 the West and Rouse labs gave new insights into the *in vivo* regulation of HJ resolutions both in human and in murine systems (Wyatt et al., 2013; Castor et al., 2013).

In Bloom's Syndrome cells, the frequency of sister chromatid exchanges is enhanced compared to normal cells due to deficiency in the dissolution pathway. Therefore BS cells can be used as a read-out to look for agents involved in the *in vivo* resolution of HJs. By introducing siRNA against endonucleases (SLX4, SLX1, MUS81, GEN1) that act in the resolution pathway into BS cells, West and colleagues found that the resolution of HJs requires two distinct pathways: one mediated by MUS81-SLX1-SLX4 complex and another pathway where GEN1 is active (Wyatt et al., 2013). Using a murine system, the Rouse lab found that SLX1 and MUS81-EME1 are epistatic in the resolution of HJs escaping the dissolution pathway, consistent with the results from West's lab (Castor et al., 2013).

However in ICL repair, it appears that only the SLX1-SLX4 interaction and not the MUS81-SLX4 interaction is required for ICLs repair and this repair involves the processing of structures other than HJs (Castor et al., 2013). Hence, it has been proposed that whereas in mitosis the resolution pathway mediated by nucleases acts when HJs escape dissolution by BLM helicase, in meiosis the resolving mechanism dominates. However, it is not yet clear which nuclease(s) resolve HJs in mammalian cells.

1.7 Impact of SLX4 scaffold on the associated nucleases

SLX4 has no obvious catalytic motifs, and instead it appears to have a more structural role, coordinating the assembly of a DNA repair complex, and interacting with three separate nucleases as described above. As mentioned in the previous section, SLX4 coordinates the nuclease activity of MUS81 and SLX1 in the resolution of HJs, by bringing the two proteins close together (Wyatt et al., 2013; Castor et al., 2013).

However, SLX4 mutants that cannot interact with MUS81 are ICL repair proficient (at least in mouse cells), and in this system, SLX4 mutants that cannot interact with SLX1 show partial defects (Castor et al., 2013). Therefore the role of SLX4 in ICL repair must involve interaction with a protein other than SLX1 and MUS81, such as XPF-ERCC1.

In humans, the XPF-ERCC1 complex is required in the NER pathway, a mechanism that repairs UV-induced lesions (Ciccia et al., 2008). Mutations on XPF or ERCC1 cause xeroderma pigmentosum (XP) an inherited disease characterized by sensitivity to UV radiation and sun-induced skin cancer (Cleaver et al., 2005). Mutations in XPF also cause striking sensitivity to ICL-inducing agents, in contrast to other NER mutants (Niedernhofer, Odijk et al. 2004). Jan Hoeijmakers lab described an XPF mutation in a progeroid syndrome XFE that caused pronounced ICL sensitivity and only mild UV sensitivity (Niedernhofer, Garinis et al. 2006). Thus it appears possible to separate the role of XPF in UV repair from ICL repair. On that note, size exclusion chromatography of cell extracts shows that the human XPF-ERCC1 is present in two distinct cellular pools. One co-elutes in a large molecular complex together with the SLX4 scaffold (Munoz et al, 2009; Stoepker et al., 2011); this fraction appears to not be involved in the NER mechanism, as human cells depleted of SLX4 are not sensible to UV light (Munoz et al. 2009; Feikairi et al. 2009). The pool of XPF-ERCC1 present in the second fraction, elutes later upon gel filtration and represents a smaller complex; most importantly it is free of SLX4 and probably represents for the NER (Muñoz et al., 2009). Therefore the pool of XPF-ERCC1 binding to SLX4 appears to be required for ICL repair only. A recent study concluded that the role of SLX4 in ICL repair involves XPF-ERCC1 only, because a fragment of SLX4 lacking amino acids 1-499, that did not interact with XPF-ERCC1, did not rescue the mitomycin-C sensitivity of

SLX4-hypomorphic MEFs (Crossan, van der Weyden et al. 2011). However, the first 499 amino acids of SLX4 also contain two ubiquitin-binding domains that are vital for ICL repair but that are not required for SLX4-XPF interaction (Kim, Lach et al. 2011; Stoepker, Hain et al. 2011).

In budding yeast the interaction of Slx4 with XPF-ERCC1 (Rad1-Rad10) is required in the single-strand annealing pathway, a mechanism involved in the repair of DNA double-strand breaks (DSBs) that occur between repetitive sequences. As shown in **Fig.4**, in this pathway the DSB undergoes an exonuclease-mediated 5'-end resection to generate 3' single-stranded DNA tails in which complementary strands of the duplicated sequence are exposed (a). The strands are then annealed (b) resulting in a structure containing 3'non-homologous tails that need to be cleaved (c) to restore the double filament (d).

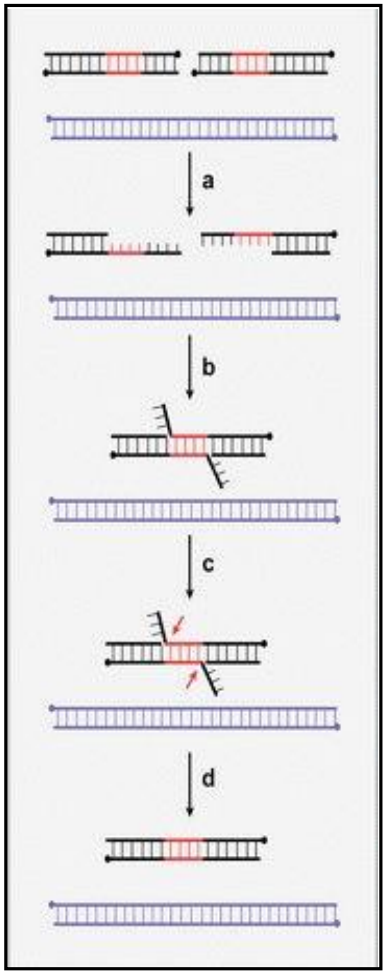

Figure 4: Schematic view of the SSA annealing pathway. (From Ciccia et al., 2008)

Experiments using the HO endonuclease to induce DSBs between repetitive elements showed that Rad1-Rad10 is the endonuclease required for the cleavage of 3' tails (Fishman et al., 1992), and similar experiments carried on mammalian cells have shown the same role for XPF-ERCC1 (Minawi et al., 2008). In yeast Slx4 was shown to interact with Rad1-Rad10 and to be essential for Rad1-Rad10 function in SSA and HR but not NER (Flott et al., 2007). Further analysis showed that Slx4 is recruited in the proximity of persistent 3' non homologous (NH) tails, and Slx4 deletion reduced SSA efficiency by impairing the removal of 3' non-homologous tail (Flott et al., 2007; Li et al., 2008). At present it is not clear why Slx4 is required for NH tail cleavage in SSA, or

what it might do to facilitate cleavage by Rad1-Rad10. It is unlikely that Slx4 recruits Rad1-Rad10 to 3' flaps, as another protein, Saw1 mediates this role (Flott et al., 2007; Li et al., 2008). Another possibility is that it might be required for the proper positioning of Rad1-Rad10 on DNA by deforming the DNA substrate or it could direct the assembly or disassembly of one of the other SSA factors.

In human cells, a direct contribution of SLX4 in the SSA pathway has not been reported yet. SLX4 binds not only to XPF-ERCC1, but also to MSH2-MSH3, a key complex in the mismatch repair (MMR) system (Svendsen et al., 2009). The MMR machinery is required to recognize and repair insertion/deletion loops (IDLs) and base-base mismatches that escape from the proofreading activity of DNA polymerases (Jiricny, 2006). MSH2-MSH3 is the heterodimer that first recognizes and binds to mismatched DNA, and starts the DNA-repairing cascade (Kunkel et al., 2005; Lyer et al., 2006; Jiricny, 2006). Interestingly, Msh2 physically interacts with Rad1-Rad10, independently of other MMR factors (Bertrand et al., 1998). Further *in vitro* and *in vivo* experiments showed that Msh2 in complex with Msh3 is required in gene conversion and single strand annealing pathway (Sugawara et al., 1997), where it most probably stabilizes structure intermediates and therefore facilitates the recruitment and cleavage activity of Rad1-Rad10 (Sugawara et al., 1997; Evans et al., 2000). It will be interesting to tie these observations together and to test the role of SLX4 in SSA in mammals.

1.8 SLX4 complex in the control of telomeres

In mammalian cells, beside the three structure specific endonucleases (XPF-ERCC1, MUS81-EME1, SLX1), there are other proteins that interact with SLX4 which are not directly involved in the repair of ICLs. Together with the discovery of the association of

MSH2-MSH3 with SLX4, the same proteomic analysis showed TRF2-RAP1 as novel factors belonging to the SLX4 complex (Svedsen et al., 2009). TRF2 and its constitutive binding partner RAP1 are part of a six-protein complex called shelterin. All the shelterin factors reside at telomeres and do not seem to localize elsewhere in the nucleus (Palm et al., 2008).

Mammalian telomeres are DNA-protein structures that protect chromosome ends from degradation and repair. Telomeres are double stranded filaments constituted of an array of TTAGGG sequence that varies in length (2-200 kb. A striking feature of these chromosome-ends structures is that the 3' filament (also called G-strand, because it is rich in guanosine) is longer than the 5' end (C strand), with an overhang of 5-500 nt. Shelterin is specific for telomeric DNA because it recognizes the TTAGGG repeats and their association with telomeres promotes the so-called "t-loop" formation. In this DNA configuration, the 3' overhang invades the duplex region of telomeric DNA and base pairs with the C-strand (Griffith et al., 1999). The purpose of the structure is to sequester the chromosome end from the DNA damage response pathway. Hence, the shelterin enables cells to distinguish natural chromosome ends from DNA breaks, avoiding the activation of DNA damage pathways that would otherwise trim the chromosomes leading to a genetic catastrophe.

The interaction between SLX4 and TRF2-RAP1 complex suggested that SLX4 might function at the level of telomeres, and this hypothesis was strengthened by the fact that an overexpressed form of SLX4 colocalizes with shelterin in a specialized HeLa cell line with extra-long telomeres (Svedsen et al., 2009). In 2013 two different laboratories showed the association of endogenous SLX4 with telomeres, by chromatin

immunoprecipitation (ChIP) and immunofluorescence (IF) (Wan et al., 2013; Wilson et al., 2013).

The length of telomeres is determined by the balanced between telomere lengthening and shortening mechanisms. In cancer cells and in some highly proliferative somatic tissues, telomeric DNA can be synthesized de novo by the ribonucleoprotein enzyme telomerase which adds telomeric repeats to the chromosome ends (Shay et al., 1997). Unlike cancer cells, in normal human somatic cells the level of telomerase activity is not sufficient to avoid telomere shortening. The negative regulation of telomere ends might involve a mechanism called “telomere trimming”, in which the t-loop structure is resolved by resolvases and leads to the formation of a truncated telomere and a telomeric circle (Pickett et al., 2011; Palm et al., 2008). Wan and colleagues noticed that a mutant deficient in the binding between SLX4 and SLX1 failed to rescue the telomere length defect due to SLX4 depletion and further *in vitro* experiments demonstrated that SLX1 is necessary for the cleavage of a D-loop (a structure that is part of the t-loop). These data led to speculation that the binding of SLX4 at telomeres is required to prevent telomere over-lengthening by recruiting the SLX1 nuclease to telomeres. Therefore, SLX4 might act as a negative regulator of telomere length (Wan et al., 2013).

1.9 Regulation of SLX4 by posttranslational modifications

Yeast SLX4 is controlled by protein phosphorylation. The Rouse lab reported that after DSBs, Slx4 is phosphorylated by the Mec1 and Tel1 kinases (ATR and ATM, respectively) on at least six Ser/Thr residues. Mutation of just one of these phosphorylation sites (Thr 113) strongly reduced the Slx4-dependent, Rad1-Rad10-

dependent cleavage of non-homologous DNA tails during single strand annealing pathway and gene conversion (Flott et al., 2007; Toh et al., 2010). Moreover, a large-scale proteomic screen of proteins phosphorylated in response to ionizing radiation, found that the murine Slx4 was also phosphorylated on consensus sites recognized by ATM and ATR (Ser/Thr – Gln) (Matsuoka et al., 2007). A smaller scale proteomic analysis also found a SQ/TQ site on human SLX4 that was phosphorylated after IR treatment (Mu et al., 2007).

There are no data yet confirming the Slx4 phosphorylation sites from the global screens, and there is no information yet on how phosphorylation might affect SLX4 function in mammalian cells. SLX4 was shown to interact with PLK1, and interesting functional connections have been made between Mus81 and Plk1 in budding yeast. The yeast orthologue of EME1, Mms4 was shown to bind to and to be phosphorylated by Cdc5, the yeast equivalent of PLK1 that is active only during the M phase of the cell-cycle (Lee et al., 2003; Clyne et al., 2003). Further analysis showed that the Cdc5-dependent phosphorylation of Mms4 was coincident with an increased activity of Mus81-Mms4 towards HJs (Matos et al., 2011); therefore the activity of the complex appears to be tightly regulated during cell cycle. Consistent with the role played by Cdc5 in the regulation of Mus81-Mms4, the human Cdc5-homologue, PLK1 was shown to be involved in the activation of MUS81-EME1 in G2/M phase in human cells (Matos et al., 2011). PLK1 phosphorylates EME1 and this modification coincides with an increase in the resolution of HJs. (Wyatt et al., 2013; Matos et al., 2011). However, it is not clear if phosphorylation of EME1 in humans is the mechanism whereby PLK1 increases HJ resolving activity. In budding yeast the Mus81-Mms4 heterodimer does not interact with Slx4 and there is no evidence that Slx4 is phosphorylated by Cdc5.

Interestingly, in human cells MUS81-EME1 becomes part of the SLX4 complex and SLX4 directly interacts with PLK1 (Svendsen et al., 2010).

SLX4 might be regulated by post-translational modifications other than phosphorylation, such as sumoylation or ubiquitination. Ubiquitination is the process through which a small polypeptide (ubiquitin) is conjugated to an internal lysine in target proteins. The conjugation is ATP dependent and involves activating enzymes (E1), conjugating enzymes (E2) and ligases (E3) (Kerscer et al., 2006). In the FA pathway on which SLX4 functions, ubiquitination is a central mechanism. The FA core complex monoubiquitinates the two components of the ID complex (FANCI/FANCD2) (Alpi et al. 2009; Meetei et al. 2003); the mono-ubiquitinated form of FANCD2 recruits the FAN1 nuclease to sites of ICLs by virtue of a UBZ4-type ubiquitin binding domains in FAN1 (Garner et al., 2011). Importantly SLX4 also has two UBZ4-type domains, that when mutated cause FA in humans (Stoepker et al., 2011; Kim et al., 2011). Our lab recently found that the first of the two tandem UBZ domains in SLX4 recruits SLX4 to DNA damage sites independently of FANCD2; therefore the ubiquitinated ligand that recruits SLX4 is unknown.

My project has involved studying the regulation of human SLX4 by phosphorylation and characterizing new factors that might be required for the ubiquitination of the SLX4 complex.

PROJECTS:

PROJECT 1: Identification of sites of SLX4 phosphorylation *in vivo*.

PROJECT 2: Identification of novel SLX4-interacting proteins.

PROJECT 3: Does SLX4 interact with MSH2-MSH3?

2 MATERIALS AND METHODS

2.1 Materials

2.1.1 Buffers and solutions

Lysis Buffer

Reagent	Final concentration
TRIS HCl (pH 7.4)	50 mM
NaCl	150 mM
EDTA (pH 8)	1 mM
EGTA (pH 8)	1 mM
Triton X-100	1%
Sucrose	270 mM
B-Mercaptoethanol	10 µl in 10 ml of final buffer volume
Protease inhibitor	1 tab
Phosphatase inhibitor	1X
Benzonase	0.2%

RIPA buffer

Reagent	Final concentration
TRIS HCl (pH 7.5)	50mM
NaCl	150 mM
NP-40	1% (v/v)
DOC	1% (v/v)
SDS	0.1% (v/v)
EDTA	2 mM
Protease inhibitor	1X
Phosphatase inhibitor	1X
Benzonase	0.2%

Tris Buffer Saline (TBS)

Reagent	Final concentration
TRIS HCl (pH 7.5)	50 mM
NaCl	150 mM
DOC	1% (v/v)
TBS-Tween	
Tween 20	0.1% (v/v)

10X TG buffer

Reagent	Final concentration
TRIS base	30 g
Glycine	144 g
Sterile water	Up to 1l

1X Transfer buffer

Reagent	Final concentration
10x TG buffer	100 ml
Methanol	200 ml
Sterile water	Up to 1l

10X TE buffer (pH8)

Reagent	Final concentration
TRIS HCl (pH 8)	100 mM
EDTA	10 mM
Autoclave	

10X LiAc

Reagent	Final concentration
Litium Acetate	1M
Filter sterilize	

1X LiAc/40%PEG-3350/0.5X TE

Reagent	Final quantity
10X LiAc	10 ml
10X TE	5 ml
PEG-3350	40 g
Sterile water	Up to 10 ml
Filter sterilize	

Z buffer

Reagent	Final quantity
Na_2HPO_4 x $7H_2O$	16.1 g
Na_2HPO_4 x H_2O	5.5 g
KCl	0.75 g
$MgSO_4$ x $7H_2O$	0.246 g
Sterile water	Up to 1000 ml
Adjust pH to 7 and sterilize	

Staining buffer for FACS experiments

Reagent	Final concentration
Propidium iodide	50µg/ml
Ribonuclease A	50µg/ml
triton X-100 in PBS	0.1% v/v

2.1.2 Kits

Kit	Source	Catalogue number
QIAquick gel extraction	QIAGEN	28704
QIAprep Spin Miniprep	QIAGEN	27106
QIAprep Spin Maxiprep	QIAGEN	12663

2.1.3 Media

Liquid media and agar plates for yeast and bacteria culture were prepared by the Kitchen Service, University of Dundee.

Luria Bertani (LB) broth

Reagent	Final concentration
Tryptone	1%
Yeast extract	0.5%
Sodium chloride	1%

When needed Ampicillin was added to a final concentration of 50 µg/ml (LB/Amp).

LB/Amp plates contained additional 2% (w/v) bacto-agar, and were stored at 4°C

YPAD

Reagent	Final concentration
Yeast extract	1%
Peptone	2%
Glucose	2%
AGAR	2%
Adenine	0.01%

Synthetic Dextrose minimal media (SD)

Reagent	Final concentration
Yeast nitrogen base without aminoacids	0.67%
Dextrose	2%

Amminoacids and bases were supplemented as required: 0.08% (w/v) each of adenine, uracil, tryptophan, histidine, arginine, and methionine; 0.12% (w/v) each of tyrosine, and lysine; 0.24% (w/v) leucine; 0.2% (w/v) phenylalanine; 0.8% (w/v) threonine). SD-plates contained additional 2% (w/v) bacto-agar.

SOC medium

Reagent	Final concentration
Yeast extract	0.5% (w/v)
Tryptone	2% (w/v)
Glucose	20 mM
KCl	2.5 mM
$MgCl_2$	10 mM
NaCl	10 mM

2.1.4 Antibodies

Antibodies against human SLX4 and human SLX1 were generated and supplied by DSTT (Division of Signal Transduction Therapy) at the Dundee University. The sequence of target proteins were fused to GST and expressed in bacteria and then used as antigens for injection into sheep. All secondary antibodies purchased were horseradish peroxidise (HP) conjugated.

Primary antibodies	Source	Catalogue number
CUL1	Invitrogen	71-8700
FBXO11	Bethyl	A301-177A
GAPDH	Abcam	Ab8245
MSH2	Bethyl	A300-452A
MSH3	Santa Cruz	SC-271080
MUS81	ImmuQuest	IQ285
RBX1	Abcam	Ab2977

SKP1	Santa Cruz	SC-5281
SLX1	DSTT*	S701C
SLX4-C	DSTT*	S714C
XPF	ThermoScientific	Ab-1 (clone 219)
UBR5	Bethyl	A303-045A
Secondary antibodies		
Mouse IgG (H + L) (HRP)	Pierce	31430
Rabbit IgG (H + L) (HRP)	Pierce	31460
Sheep IgG (H + L) (HRP)	Pierce	31480

*Cloning team, University of Dundee

2.1.5 Plasmids

Name	Source	Catalog number
MSH2	DSTT*	19058
MSH3	DSTT*	19059
SLX4	DSTT*	16417
pDONOR	Life technology	11798-014
pDEST22	Life technology	-
pDEST33	Life technology	-

*Cloning team, University of Dundee

2.1.6 Small interfering (si)RNA oligos

UBR5 siRNAs duplexes were purchased from Eurofins-MWG.

Target	Oligo number	Target sequence (sense)
UBR5	1	GCA CUU AUA UAC UGG AUU A
UBR5	2	GAU UGU AGG UUA CUU AGA A
UBR5	3	GGU CGA AGA UGU GCU ACU A

2.1.7 Oligonucleotides

All the oligonucleotides listed below are flanked with attB oligos for Yeast Two Hybrid analysis, and they were synthesized by the Oligonucleotide Synthesis Service, University of Dundee.

MSH2

Fwd_attB1_MSH2: 5' - ACA AGT TTG TAC AAA AAA GCA GGC TTC ATG GCG GTG CAG CCG AAG – 3'

Rev_attB2_MSH2: 5’ - AC CAC TTT GTA CAA GAA AGC TGG GTT CGT AGT AAC TTT TAT TCG TGA AAT GAT TTC – 3’

MSH3

Fwd_attB1_MSH3: 5’ -ACA AGT TTG TAC AAA AAA GCA GGC TTC ATG TCT CGC CGG AAG CCT GC-3’

Rev_attB2_MSH3: 5’ - AC CAC TTT GTA CAA GAA AGC TGG GTT ATG AAG AAG AGA AGT CTG TGT TTC TTC CAT GTT G – 3’

SLX4

Fwd_attB1_SLX4: 5’- ACA AGT TTG TAC AAA AAA GCA GGC TTC ATG AAA CTG AGT GTG AAT GAG GCT CAG CTA GGC - 3’

Rev_attB2_SLX4: 5’- AC CAC TTT GTA CAA GAA AGC TGG GTT GTT CCG CTC CAC CTT CTT CTT GCC CCG AGG CTG - 3’

Fwd_attB1_SLX4-X2/X4: 5’- ACA AGT TTG TAC AAA AAA GCA GGC TTC ATG GAG GTT GGC CCC CAG CTC CTG CTT CAG GCT - 3’

Rev_attB2_SLX4-X1: 5’- AC CAC TTT GTA CAA GAA AGC TGG GTT GTT CAA GGT TCG GCC GCC CCT GTC CGG GTG CTT - 3’

Rev-attB2_SLX4-X2: 5’- AC CAC TTT GTA CAA GAA AGC TGG GTT GTT GGC AAT AGG CAC CTG TTC

GCA CAG GTG AAC - 3’

Rev-attB2_SLX4-X3/X4: 5’- AC CAC TTT GTA CAA GAA AGC TGG GTT CAA GGT TCG GCC GCC CCT GTC CGG CTC CTT GTC - 3’

Fwd_attB1_SLX4-M1: 5’- ACA AGT TTG TAC AAA AAA GCA GGC TTC ATG ACT GAC TCA GAG GGC AAA CCA TGG GAG GAG - 3’

Fwd_attB1_SLX4-M2: 5’- ACA AGT TTG TAC AAA AAA GCA GGC TTC ATG CTC TCC CTC GGG CTG CTG GTT GCT GAC TTT GG - 3’

Rev_attB2_SLX4-M: 5’- AC CAC TTT GTA CAA GAA AGC TGG GTT GTT CAT CGG CGT TAT GGG CAC TTT GGG GGG CAA - 3’

Fwd_attB1_SLX4-S: 5’- ACA AGT TTG TAC AAA AAA GCA GGC TTC ATG CAG ACC TAC AAG CCT TCA AGG GCA GGG GTC - 3’

Rev_attB2_SLX4-S: 5’- AC CAC TTT GTA CAA GAA AGC TGG GTT GTT CCG CTC CAC CTT CTT CTT GCC CCG AGG CTG - 3’

2.1.8 Yeast and bacterial strains

Name	Organism	Source	Catalog number
MAV203	*S. cerevisiae*	Life technology	11281-011
TOP10	*E. coli*	Invitrogen	C4040-10
DH5α	*E. coli*	DSTT	-

2.2 Methods

2.2.1 Determination of protein concentration

Protein concentrations were measured by the Bradford method (Bradford 1976). A standard curve was prepared according to the manufacturer's protocol, by adding increasing amount of BSA to a final volume of 0.1 ml with water, and then mixing with 0.9 ml Bradford reagent. The mixture was allowed to stand at room temperature for 5 min. The optical density of the standards was measured at 595 nm (OD_{595}) in 1.5 ml plastic cuvettes against a reference cuvette containing water (0.1 ml) and Bradford reagent (0.9 ml). This was used to construct a standard curve that was employed to determine protein concentrations of cell lysates. On average the linear range of protein Bradford measurements lies between OD_{595} 0.1 and OD_{595} 0.7. Cell lysates were diluted so that the OD_{595} lay in this range. Bradford measurements were performed in triplicate.

2.2.2 Determination of DNA concentration

The absorbance of DNA in aqueous solutions was measured in a disposable UVette at 260 nm with a Biophotometer, using the OD_{260} of sterile water as zero.

2.2.3 DNA sequencing

Sequencing of either plasmid DNA or PCR product DNA was performed by The Sequencing Service, School of Life Science, University of Dundee, using DYEnamic ET terminator chemistry (Amersham Pharmacia Biotech) on Applied Biosystems automated DNA sequencers. For DNA containing high GC content (typically > 75%), 10% (v/v) of GC-melt solution (Clontech) was added to the sequencing reaction.

2.2.4 Immunoprecipitation (IP)

2.2.4.1 Conjugation of antibodies to protein-G Sepharose

The required volume of protein-G Sepharose was washed 3 times in PBS then adjusted to a 50% (v/v) slurry in PBS before addition of antibodies. The antibody/Sepharose mixture was mixed on a platform shaker at 4°C. After 60 min, the beads were washed 3 times with PBS. Generally, 2 µg of antibody was conjugated to 10 µl of settled protein-G Sepharose beads.

2.2.4.2 Immunoprecipitation of proteins from native cell lysates

Generally 2µg coupled antibody was used per 1 to 3 mg extract. The antibody-bead conjugate was incubated with cell extract for 2 hours at 4 °C on a shaking platform or a roller depending on the size of the tube used. The supernatant was removed and the beads washed three times with 500µl of lysis buffer and a final wash was done with 500µl of Tris HCl (50mM) and 270 mM of Sucrose. Immunoprecipitates were denatured in lithium dodecyl sulphate (LDS) sample buffer (1x) and β-mercaptoethanol (5% v/v). Samples were boiled at 95°C for 5-10 min before loading onto

polyacrylammide gels.

2.2.5 Separations of proteins by sodium dodecyl sulphate (SDS)-polyacrylammide gel

Two SDS-PAGE systems were used in this thesis depending on the experiment. The first one was NuPAGE 4-12% Bis-Tris pre-cast gels coupled with the BioRad system for electrophoresis transfer. Electrophoresis was performed using electrophoresis buffer at constant voltage of 150V for 90 to 105 min, depending on the experiment. Invitrogen Bis-Tris gels were run in Novex NuPAGE 3-[N-morpholino] propane sulphonic acid (MOPS) running buffer.

The second system used was the ATTO self-pour gel system for gel electrophoresis coupled with the BioRad system for electrophoretic transfer. Slab gels for the ATTO system were poured between glass plates using separating gel consisting of 0.375M Tris-HCl pH 8.8, 0.1% (w/v) SDS, 10% (w/v) acrylammide/o.4% (w/v) N,N'-methylene bisacrylammide and 0.075% (w/v) ammonium persulphate. Polymerisation was initiated by the addition of 0.1% (v/v) tetramethylethylenediamide (TEMED). Isopropanol was then layered carefully over the acrylamide solution and polymerisation allowed to continue for at least 15 min. The isopropanol was removed and stacking gel comprising 0.125M Tris-HCl (pH 6.), 0.1% (w/v) SDS, 3% (W/v) acrylamide/0.08% (w/v) N, N'-methylene bisacrylamide, 0.075% (w/v) ammonium persulphate and 0.1% (v/v) TEMED, was poured onto the seprarating gel top and a 14-well comb was added prior to polymerisation and left to set for at least 10 min. Electrophoresis was performed using electrophoresis buffer at a constant voltage of 150V for 90 min.

2.2.6 Staining of protein gels

To visualize proteins after SDS-PAGE, gels were stained Colloidal Coomassie Blue staining solution for 60 to O/N at room temperature with a continual agitation on a rocking platform. Gels were destained with water, using several changes until the background staining was greatly reduced.

2.2.7 Western blotting

Protein gels were assembled into a gel-membrane sandwich as described in the manufacturer's protocol. Nitrocellulose membrane was placed on a gel, this assembly was posed between two sponges. All components were pre-soaked in transfer buffer. This assembly was loaded into a BioRad Mini-Cell tank filled with transfer buffer, and proteins were transferred to nitrocellulose at 105V for 105 min. The nitrocellulose membrane was blocked in TBS-Tween 0.15% containing either skimmed milk (5% w/v) or BSA (4% w/v) for 1 h at room temperature. Primary antibodies were diluted in TBS-Tween containing either skimmed milk (5% w/v) or BSA (4% w/v) and, depending on the efficiency of the antibody, incubated for 1-2h at room temperature or 4°C O/N. The membrane was washed 3 times for 10 min each with TBS-Tween 0.15%, incubated with secondary antibodies conjugated to horseradish peroxidase (HP) (all secondary antibodies were used at 1:5000 dilutions in TBS-T containing either skimmed milk (5% w/v) or BSA (4% w/v)) for 1h at room temperature. After the three round of washing, the membrane was developed with enhanced chemiluminescence reagent (ECL). To detect secondary antibodies conjugated with HP, ECL reagents 1 and 2 were mixed in equal volumes and 1 ml of this mix was added to each blot for 1min. The membrane was then placed in a clean piece of polythene roll in an autorad cassette. The

membrane was then exposed to Medical X-Ray Film (Konica Minolta) and developed in an automatic processor.

2.2.8 In gel digestion of proteins for Mass spectrometric analysis

To minimise keratin and other exogenous contaminations, all manipulations of gels for mass spectrometry analysis were prepared under a laminar flow hood. Protein bands were excised from a colloidal Coomassie stained gel, using a sterile scalpel. Gel pieces were washed with 0.5 ml each of 50% acetonitrile/water 0.1 M NH_4HCO_3 and 50% Acetonitrile/50 mM NH_4HCO_3. All washes were performed on a Vibrax shaking platform for 10 min. All liquid was removed between washes. Proteins were then reduced with 0 mM DTT in 0.1 M NH_4HCO_3 (45 min, 65°C) and alkylated with 50 mM iodoacetamide in 0.1 M NH_4HCO_3 (30 min at room temperature). Gel pieces were then repeatedly washed with 0.1 M NH_4HCO_3 and 50% Acetonitrile/50 mM NH_4HCO_3. Once colourless, the gel pieces were shunk with 0.3 ml acetonitrile for 15 min, the acetonitrile was then removed and a Speed-Vac was used to dry the gel pieces. The latter were then swollen in 25 mM Triethylammonium bicarbonate with 5 µg/ml of trypsin and incubated over-night at 30°C on a shaker. After 12 h an equivalent volume of acetonitrile was added to the digest and incubated for further 15 min. The supernatants were transferred to a clean tube and concentrated to dryness by Speed Vac. Meanwhile 100 µl 50% acetonitrile/25% formic acid was added to the gel pieces. This second extraction was combined with the dried first extract. The samples were then stored at 20°C.

2.2.9 Mass spectrometry

Liquid chromatography-mass spectrometry (LC-MS) analysis was performed by Dr. David Campbell and Dr. Robert Gourlay. The reconstituted tryptic peptides were injected onto a Dinex 3000 nano liquid chromatography system coupled to a Thermo-Electron LTQ-orbitrap mass spectrometer. Data files (raw files) were converted to MSM files which were then submitted to the in house Mascot server. Peptide mass fingerprinting analysis was performed using OLMAT (http://www.proteinguru.com/MassSpec/OLMAT).

2.2.10 Cell cycle analysis

2.2.10.1 Elutriation of NB4 cells

This protocol was used to enrich for cells at G1, S, and G2/M cell cycle phases by centrifugal elutriation.

Preparing the elutriator

With a high flow of elutriation buffer, i.e. Flow Setting (FS) of ~150, all air bubbles were ejected from tubing by squeezing and releasing the tubing at ~10 psi of backpressure. Bubbles were then removed from chamber by repeating the same procedure with the chamber held upright. Fow was turned off. The Trap Valve was turned to Pos 1 and the Inject Valve to Pos 1. To remove bubbles trapped in the elutriation chamber the centrifuge spin was set at 1000 rpm. Centrifuge and flow rate were then stopped.

Elutriation

Cells were pelleted (1000 rpm, 4 min), resuspended in 5 mL elutriation buffer and transferred to 50 mL falcon tube. They were then loaded into syringe and pass slowly through 18 gauge needle into same falcon tube to produce monodispersion. This was repeated three times.

Next the centrifuge was set at 1800 rpm and FS to 102. If the back pressure increased above 5 psi, centrifuge was stopped, and tubes repositioned.

Cells were loaded into syringe, leaving a small aliquot in 50 mL tube for asynchronous control.

Next bubble trap was removed from flow (Trap Valve Pos 1) and the syringe inserted into luer lock. The Inject Valve was turned so that the bubble trap is isolated (Inject Valve Pos 2) and only after that, cells were slowly injected into the bubble trap. The Inject Valve was then closed (Inject Valve Pos 1) and the bubble trap reconnected to the flow (Trap Valve Pos 2). Flow was adjusted to ensure that cells filled the chamber. After all cells were loaded into the chamber, Trap Valve was switched to Pos 1. For each fraction, cells were collected into 50 mL falcon tube. For NB4 cells, FS was: 112 (G1), 118, 122 (S), 126, 130, and 150 (G2/M). Spin was then stopped, and the last 50 mL fraction ("Post") collected. Elutriation buffer was replaced with 70% ethanol to clean the tube and let it flow until all liquid was removed.

Notes

- **Trap Valve**
    - Pos 1: The T-valve is turned such that the flow goes through the bubble trap
    - Pos 2: Bypass the bubble trap
- **Inject Valve**

- Pos 1: The “OFF” end is pointing towards the luer lock.
- Pos 2: The “OFF” end is pointing towards the T junction with the peristaltic pump.

2.2.10.2 Cell cycle analysis by FACS: Propidium Iodine stained cells

This protocol has been used to stain DNA deriving from cells collected during time points in cell-cycle experiments. The pellet deriving from cells collected during timepoints, was resuspended in 1 ml of 70% of cold ethanol and left at least for 30 min at room temperature. Cells were washed twice in PBS + 1% BSA or FCS (Fetal Calf Serum) and filtered through filcons 50 µm, BD (Biosciences) in FACS tubes to get rid of clumps of cells. Cell were then pelleted and resuspended in 1 ml of staining buffer, incubated at room temperature protected from light for at least 20 min, and analyzed by flow cytometry. Live cells were gated on the flow cytometer using forward scatter and side scatter parameters. DNA was detected in the FL2-H channel. FL2-W and FL2-A were used to distinguish single cells. Cell numbers at different cell-cycle stages were measured on FlowJo.

2.2.11 Yeast two hybrid assay (Gateway cloning)

2.2.11.1 attB flanked PCR amplifications of the fragments

REAGENTS	**QUANTITY (final concentration)**
Platinum SuperMix HiFi	45 µl
Template	10 ng
Primers flanked by attB sites	1 µM

TEMPERATURE	TIME	
94°C	2 min	
94°C	30 sec	25 cycles
55°C	30 sec	
68°C	3 min	
68°C	10 min	
6°C	O/N	

The PCR products were then run into an agarose gel electrophoresis and bands visualized under UV light. Gel pieces at the correct molecular weight were cut, inserted into a 15 ml falcon tube, and DNA was extracted from the agarose by using a QIAquick Gel Extraction Protocol. The concentrations of the fragments were checked on a Nanodrop.

2.2.11.2 BP reaction

attB flanked PCR products were introduced into an expression vector (pDONOR) in a reaction mediated by BP clonase enzyme, this yielded to a pENTR vector containing the fragments of interest. The pDONOR carried a spectinomycin resistance gene for further selection in *E. coli*.

REAGENTS	QUANTITY (final concentration)
pDONOR	150 ng
attB flanked PCR	100 ng
TE buffer pH8	up to 10 µl
BP clonase enzyme	2 µl

The reaction was mixed by vortex, and incubated at 25°C for 20h. Next, 1µl of proteinase K solution was added, and incubated at 37°C for 10min.

2.2.11.3 Transformation of pENTR into TOP10 E.coli strain

A maximum of 2.5 µl of the BP recombination reaction was added into a chilled electroporation cuvette , next 100 µl of TOP10 cells were added and gently mixed. Cells were electroporated by choosing EC2 (bacteria) program + pulse once. For the recovery of the cells, 500 µl of SOC medium was added into the mix, pipetted gently and transferred into a 1.5ml eppendorf tube. Cells were incubated at 37°C for 30 min in a thermomixer and finally plated on a LB + spectinomycin plate (to select positive clones) and incubated at 37°C O/N.

The day after, each colony was inoculated in 3 ml LB + spectinomycin medium and incubated at 37°C O/N. DNA was purified by using a QIAprep Spin Miniprep kit and the correct sequence of the constructs was verified by restriction enzymes and sequence analysis.

2.2.11.4 LR reaction

pENTR vector was recombined with a destination vector (pDEST) to create an expression clone containing fragments of interest. pDEST22 is the GAL4 Activation Domain, and pDEST32 is the GAL4 DNA Binding Domain containing destination vector. pDEST22 encodes ampicillin resistance, whereas pDEST32 carries a gentamycin resistance gene for further selection in *E. coli*.

REAGENTS	**QUANTITY (final concentration)**
pENTR	150 ng
pDEST32/22	150 ng
TE buffer pH8	up to 10 µl
LR clonase enzyme	2 µl

The reaction was incubated at 25°C for 1/2hours, transformed into TOP10 and subsequently plated onto gentamicin plates (10µg/ml).

2.2.11.5 Transformation of pDEST22 and pDEST32 into MAV203 cells

A colony of MAV203 was inoculated in 10 ml of YPD and incubated overnight at 30°C. The next day the OD_{600} of the culture was determined and cells were diluted to an OD_{600} of 0.4 in 50ml of YPD and let them grow additional 2-4 hours. Cells were then pelleted at 2500 rpm and resuspended in 40ml 1X TE; pelleted a second time at 2500 rpm and resuspended in 2ml of 1X LiAc/0.5X TE.

Finally cells were incubated at room temperature for 10 minutes.

For each transformation 1 µg of plasmid DNA and 100 µg of denatured sheared salmon sperm DNA was mixed together with 100 µl of the yeast suspension. Next, 700 µl of 1X LiAc/40% PEG-3350/1X TE was added to the cells and mixed well. The solution was incubated at 30°C for 30 minutes. After that, 88 µl of DMSO was added, mixed well, and cells were subjected to heat shock at 42°C for 7 minutes. Cells were then centrifuged for 10 seconds, the supernatant removed, and the pellet resuspended in 1 ml 1X TE and re-pelleted. After removing the supernatant from the second centrifugation, the pellet was resuspended in 50/100 µl TE and plated on –LEU, -TRP plates to select the insertion of both of pDEST plasmids. Single colonies were picked and a drop test performed on –LEU, -TRP plates. After that, cells were replica plated on YPAD containing a nitrocellulose membrane for the X-gal assay, –LEU, -TRP, +HIS plates to test for the activation of *HIS3* reporter gene.

2.2.11.6 X-gal assay

For each membrane, 10 mg X-gal was dissoved in 100 µl N,N-dimethyl formamide (DMF). The solution was combined with 60 µl β-mercaptoethanol and 10 ml Z-buffer. Two round 125-mm Whatman 541 filter papers were stuck in a 15 cm petri dish, and saturated with 8ml of the X-gal solution. Any air bubbles were removed. Using forceps, the membrane was removed from the surface of the YPAD plate and completely immersed in liquid nitrogene for 20-30 seconds. The frozen membrane was placed on top of the soaked Whatman filters colony side up. Any air bubbles and excess buffer were removed. Plates were then covered and incubated at 37°C up to 24 hours.

2.2.12 Transformation of Escherichia coli cells (DH5 α)

For each transformation, competent *E. Coli* cells (50 µl) from 80°C glycerol stocks were thawed on ice. Plasmid DNA (around 50 ng) was added to the cells, mixed gently, and incubated on ice for 5-20 min. To facilitate the uptake of DNA, cells were heat-shocked with an incubation at 42°C for 30s, then the cells were placed back on ice for further 2 min. Plasmids requiring ampicillin selection were streaked directly onto LB/Amp agar plates. For plasmids requiring any other selection, LB (1 ml) was added to the cells and the cells were allowed to recover at 37°C for 1 h in a shaking incubator, before being plated onto LB agar plates. Cells were let growing on the plates O/N at 37°C.

2.2.13 Preparation of plasmids from bacteria

To prepare small amounts of plasmid DNA in microgram quantities (termed 'mini-prep'), DH5α *E. coli* cells were transformed with plasmid DNA, and a single colony was inoculated in LB/Amp (5 ml). The transformed cells were grown in LB media containing

appropriate antibiotics to stationary phase by incubation at 37 °C overnight in a shaking incubator. After centrifugation in an AllegraTM6R bench-top centrifuge (Beckman), plasmid DNA was extracted from the cell pellet by sequential lysis, precipitation, binding to Qiagen anion exchange column and elution on an automated Qiagen BioRobot 9600 using the QIAsoft 3.0 software program, by the DNA Sequencing Service (University of Dundee). The DNA was eluted in sterile water (100 µl) and typically yielded 100-300 µg/ml plasmid DNA.

To prepare larger quantities of plasmid DNA, 'maxi-preps' were performed using the Qiagen DNA Maxi Kit. A single bacterial colony, transformed with the relevant construct, was used to inoculate LB (250 ml) containing the appropriate antibiotic. After an overnight incubation at 37 °C, the cells were pelleted by centrifugation at 3,000 rpm for 10 min in a J-6 Beckman centrifuge. Plasmid DNA was purified according to the manufacturer's instructions. Overnight cultures of 250 ml typically yielded 0.5-1 mg plasmid DNA.

2.2.14 Restriction digests of DNA

Restriction digests were performed at 37 °C for 1-2 hours. Restriction enzymes were used according to the manufacturer's protocol. Typically, 100 ng of DNA was digested with the relevant restriction enzyme buffer, water, BSA (at final concentration of 100 µg/ml) and restriction enzyme (generally 1 unit of enzyme per 1 µg of DNA).

2.2.15 Mammalian cell culture

All media and buffers used for mammalian cell culture were pre-warmed to 37°C prior to use and all procedures were carried out under aseptic conditions compliant with

biological safety Category-2 regulations. Unless otherwise indicated, cells were cultured and maintained at 37oC in a 5 % CO2 water-saturated incubator. Cells were grown until 80-90 % confluency before splitting for routine maintenance.

2.2.16 Human embryonic kidney 293 (HEK293) cells

HEK293 cells were purchased from the European Collection of Cell Cultures (Salisbury). They were cultured in 150 cm^2 flasks (for routine passaging) or on 10 cm^2 plates in DMEM supplemented with 10 % (v/v) fetal bovine serum (FBS) and 1 % (v/v) penicillin/streptomycin stock solution (10,000 units penicillin and 10 mg streptomycin per ml). For passaging of cells, culture medium was aspirated, cells were washed once with sterile Dulbecco's phosphate buffered saline (PBS) and 2 ml of sterile trypsin/EDTA was added per flask. After the cells detached from the surface of the flask, they were resuspended to a final volume of 10 ml in complete medium and clumps of cells were broken up by passing though a narrow- bore pipette several times. 2 ml of this cell suspension was used to seed a 150 cm^2 flask to maintain stocks in 20 ml of complete medium.

2.2.17 Cell freezer stocks

Cell stocks were stored at -196 °C in liquid nitrogen; when necessary, growing cells were frozen down to ensure a constant supply. Cells to be frozen for storage were allowed to grow to 80% confluence; after washing with PBS, trypsin was added to detach cells. Harvested cells were then washed, to remove trypsin, in an excess of normal growth media by centrifugation at 1000 rpm for 5 min. The supernatant was removed and after tapping the tube to loosen up the pellet, cells were resuspended in

cryogenic storage media (50 % FCS, 10 % DMSO, 40 % DMEM). Cells were resuspended so that 1 ml cryogenic storage media contained the same number of cells that would have been passaged into a new dish. Aliquots of cell suspension (1 ml) were stored in 1.5 ml cryogenic screw top vials (Corning) at -80°C in an insulated box for 24 h, before transfer to the liquid nitrogen cell freezer. This is because, to ensure viability during storage at - 196°C, cells must be allowed to cool at a rate slow enough to allow the cells time to dehydrate but fast enough to prevent excessive dehydration damage. A cooling rate of -1°C to -3 °C per minute is satisfactory for most animal cell cultures.

2.1.9 Transfection of HEK293 with siRNA

siRNAs were dissolved in 5X siRNA buffer (Dharmacon) and made up with water free from RNase and DNase according to manufacturers instructions. For a single transfection experiment in a 10 cm^2 plate, confluent HEK293 cells were trypsinized and approximately $4x10^6$ cells were seeded onto a 10 cm^2 plate. The cells were allowed to adhere to the plates and recover from the trypsinization process for 24 h before transfection. For each 10 cm^2 plate, 50 µl of Hiperfect transfection reagent was mixed with proper amount of siRNA (usually from 5 up to 100nM) in a 1.5 ml autoclaved eppendorf tube and the mix was added to 500 µl of Dulbecco's medium. The tube was then vortexed and the solution incubated for 10 minutes at room temperature. After that the mix was evenly added into the plate and cells were incubated at 37°C. After 24h the medium was changed with fresh Dulbecco's medium + FBS, pen/strep, L-glutammine.

2.1.10 Cell treatment with genotoxins

Cells were treated with a variety of genotoxins at a range of concentrations as indicated. Cisplatin and camptothecin were dissolved in DMSO to make 1 M stock solutions, hydroxyurea was dissolved in Milli-Q water to make 1 M stock solutions, and mitomycin-C was dissolved in Milli-Q water to make a 0.5 mg/ml stock solution. All the solutions were stored at -20°C. Ionising radiation was delivered using a ^{137}Cs radiation source at a delivery rate of 3 Gy/min.

3 IDENTIFICATION OF SITES OF PHOSPHORYLATION IN HUMAN SLX4

3.1 INTRODUCTION

At the outset of this work, there was some limited evidence from proteomic screens to suggest that the human and mouse orthologues of SLX4 are phosphorylated on S/T-Q sites, the consensus for ATM/ATR (Flott et al. 2007; Toh et al. 2010; Matsuoka et al. 2007; Mu et al. 2007), in response to DNA damage. Moreover, the Rouse lab identified several S/T-Q sites of phosphorylation in yeast SLX4 (Flott et al. 2007; Toh et al. 2010). All the sites are listed in **Table 2**.

SLX4 PEPTIDE	PHOSPHO RESIDUE/S IDENTIFIED	ORGANISM
SPMTQETTKNDTER	Thr72	Budding yeast
NKDVDKSCNPVSTSHPDLGGSNIEENIFINTQIQSR	Thr113	Budding yeast
GDSTSSQEYGNGLEPQQPVGNVVGEDIELAVGTR	Ser335	Budding yeast
IRDTQSAVNFLSLpSQVMDDK	Thr319, Ser329	Budding yeast
DNQESSQQR	Ser289	Budding yeast
R.TMLETAQQFSVIMPHTQPITLGAFDSGR.Q	Thr 1107	Mouse
CSSQTQ	Thr 1273	Human

Table 2: Previously reported sites of phosphorylation in Slx4.

As mentioned in the Introduction, in budding yeast the phosphorylation of SLX4 is very important for the modulation of its activity in single strand annealing (Flott et al. 2007). This function could have been conserved through the evolution and other phosphorylation-dependent functions could have arisen. Therefore, I performed an analysis to find the key residues on human SLX4 that are phosphorylated *in vivo,* and to understand their impact on the SLX4 activity. For my project I used an approach

that combined an immunoprecipitation of the endogenous SLX4 with phospho-mapping analysis of the protein sequence by mass-spectrometry.

3.2 RESULTS

3.2.1 Optimization of SLX4 yield prior to immunoprecipitation

In order to find the optimal conditions to immunoprecipitate (IP) SLX4, I first lysed different human cell lines (**Table 3**) and checked the expression levels of SLX4 by western blot (**Fig.5**)**.**

SLX4 was most abundant in HEK293, Ramos, and U2OS cells. I decided to choose HEK293 cells to go forward. It is important to underline that all cell lines expressed SLX4 (data not shown), but in some of cell lines shown in Fig. 1, the abundance of the protein was low that SLX4 was not detectable at the low exposures necessary to avoid overexposure of the stronger signals.

I next aimed to map SLX4 phosphorylation sites before and after exposure of cells to agents that induce DNA damage. I first optimized the extraction of SLX4 during cell lysis to ensure that I could immunoprecipitate as much of the total SLX4 as possible. I first determined which lysis conditions would yield high levels of soluble SLX4. In **Fig.5** lysis buffer contained only 150mM NaCl and not all the protein became soluble (data not shown), suggesting that a fraction of SLX4 was still bound to the chromatin. Therefore, I tried supplementing the buffer with increasing concentrations of salt (NaCl) with or without addition of benzonase, a genetically engineered endonuclease that degrades both DNA and RNA. As shown in **Fig.6**, the amount of protein in the pellet diminished with increasing salt concentrations; moreover, the benzonase did not

seem to affect the release of the protein. Hence, supplementing the lysis buffer with 300mM NaCl - without benzonase - gave the best conditions to release SLX4 from the chromatin pellet. I used these lysis conditions to immunoprecipitate SLX4 from HEK293 cells in subsequent experiments.

NUMBER	ORGAN	CELL LINE	NORMAL/CANCER	CELL TYPE
1	COLON	HCT116	C	epithelial
2	KIDNEY	HEK293	N	epithelial
3	BRAIN	U87-MG	C	epithelial
4	BRAIN	SK-N-MC	C	epithelial
5	LUNG	H1299	C	epithelial
6	LUNG	W138	N	fibroblast
7	PROSTATE	PNT1A	N	epithelial
8	PROSTATE	DU145	C	epithelial
9	OVARY	SK-OV-3	C	epithelial
10	BREAST	MCF7	C	epithelial
11	SKIN	A431	C	epithelial
12	SKIN	HaCats	N	keratinocytes
13	LIVER	HEPG2	C	epithelial
14	CERVIX	HeLa	C	epithelial
15	BONE	SK-ES-1	C	epithelial
16	BONE	U2OS	C	epithelial
17	BLOOD/LYMPHOID SYSTEM	RAMOS	C	B lymphocyte
18	BLOOD/LYMPHOID SYSTEM	THP1	C	monocyte

Table 3: List and origin of human cell lines used to test expression of SLX4.

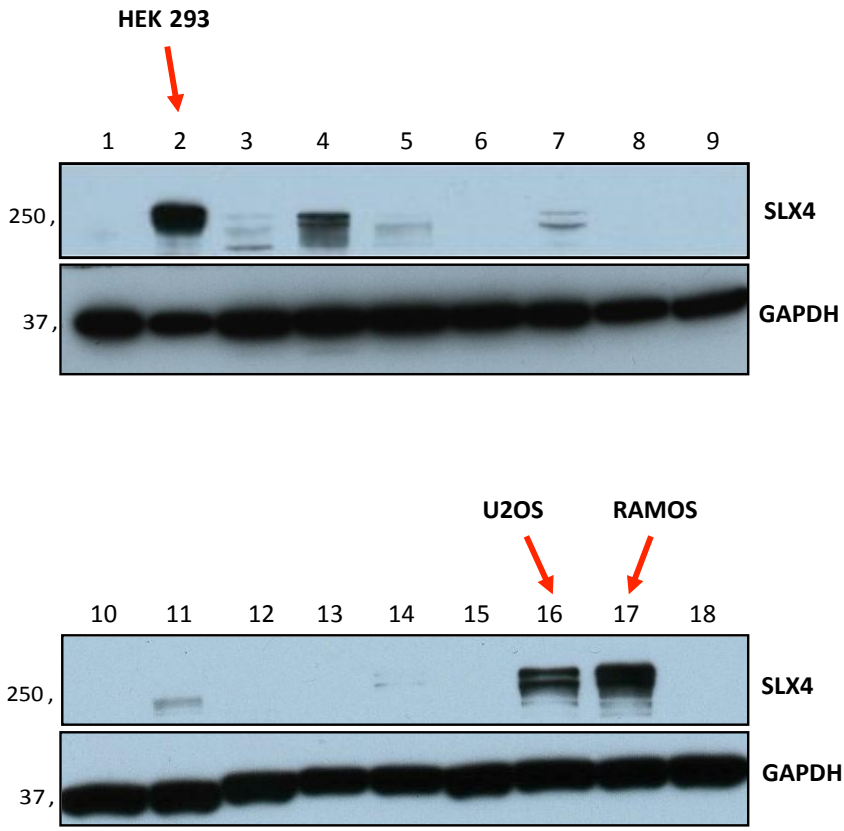

Figure 5: Expression levels of SXL4 across a panel of cell lines listed in Table1.

Western blot analysis of SLX4 expression in the cell lines listed in Table 1. Cells were lysed in buffer containing 150 mM. GAPDH was used as loading control. Supernatant shown. Red arrows highlight the three cell lines that expressed the highest levels of SLX4 which are HEK293, U2OS and RAMOS cells.

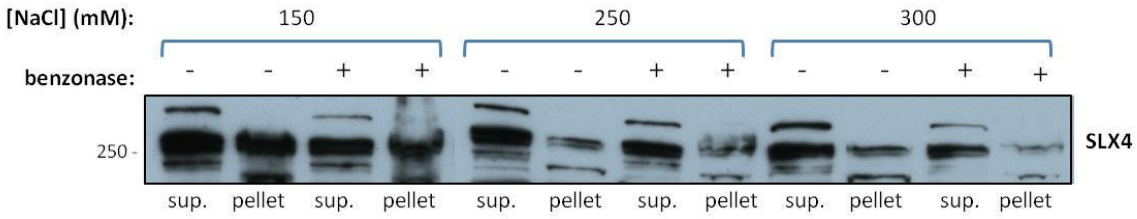

Figure 6: Testing different lysis conditions for SLX4 extraction from HEK293 cells.

HEK293 cells were lysed in lysis buffer with the supplements indicated. “Sup” denotes supernatant from centrifugation of lysates, pellet denotes the pellet remaining after centrifugation.

3.2.2 Large scale immunoprecipitation and phospho-site mapping of SLX4

It is known that human SLX4 is involved in the repair of DNA interstrand crosslinks (ICLs), and cells defective in SLX4 are hypersensitive to agents that induce ICLs. Therefore I compared phospho-sites of endogenous human SLX4 before and after treating cells with the DNA crosslinking agent mitomycin C (MMC) via immunoprecipitation and mass spectrometry analysis. MMC induces the activation of the DNA damage response (DDR), which is orchestrated by the activity of phosphoinositide 3-kinase related kinases (PIKKs) ATM and ATR (Cimprich and Cortez 2008), which have been reported to target murine and yeast Slx4 (Flott et al. 2007; Toh et al. 2010; Matsuoka et al. 2007). For cell lysis, I used the optimized conditions described above, and immunoprecipitates were resolved using SDS-PAGE, and subjected to Coomassie staining and western blotting in parallel. As shown in **Fig.7**, SLX4 was detected by western blotting in both of the SLX4 precipitates but not in the IgG control precipitate. Although in the western blot the SLX4 band migrated to the expected molecular weight, Coomassie staining showed a range of bands that could correspond to SLX4 and perhaps modified forms of this protein. In both SLX4 immunoprecipitates (plus and minus MMC), there were two strong bands that were not in the IgG control, and that could have been SLX4. One migrated at 250 kDa (C and 3 and the second ran slightly more slowly at around 300 kDa (A and B). Neither of these bands was perfectly superimposable on the SLX4 western blot (**Fig.7**). Therefore, it is likely that the Coomassie band corresponding to SLX4 was a weaker band in between the two strong bands. Nonetheless, the immunoprecipitation worked, as tryptic petides corresponding to SLX4 were identified in both bands by mass

spectrometry analysis. The lower migrating bands (C and D) were not only identified as SLX4 with protein coverage of 40% and 45% for untreated and treated cells respectively, but multiple phospho-sites were detected.

My first interest was to look for phospho-peptides with SQ or TQ motifs as these are the preferred motifs for the ATM/ATR kinases (Kim, Lim et al. 1999) and I expected that any such phospho-peptides would be enriched after DNA damage. Three SQ/TQ phospho-sites were identified in SLX4 where the abundance ratio between cells treated with MMC versus untreated cells was above 1, SRDCS**SQ**TQISSLR, GGT**SQ**VGSPTLLSPAVPSK, EGSLPHSDDAGDYEQLFSS**TQ**GEISEPSQITSEPEEQSGAVR (**Fig.8**). None of them belongs to known SLX4 domains, but the first peptide is conserved among closely related eukaryotes (**Fig.8**).

As well as ATM/ATR phospho-dependent sites, I identified several constitutive Ser-Pro (SP) and Thr-Pro (TP) sites which could be phosphorylated by any of the proline-directed kinases in cells including MAP kinases or cyclin-dependent kinases (CDKs) for example (**Fig.9**). **F**our phospho-sites (contained in peptides 11, 14, 17, 20) conform to the most stringent consensus sequence (S/T-P-X-R/K) for CDKs (Holmes and Solomon 1996; Songyang, Lu et al. 1996). Many of the members of this class of protein kinase are activated at specific points of the cell cycle to enable specific cell cycle transitions by phosphorylating cell cycle-specific targets (Vermeulen, Van Bockstaele et al. 2003). Phosphorylation of SLX4 in this manner raises the possibility of cell cycle dependent regulation of SLX4.

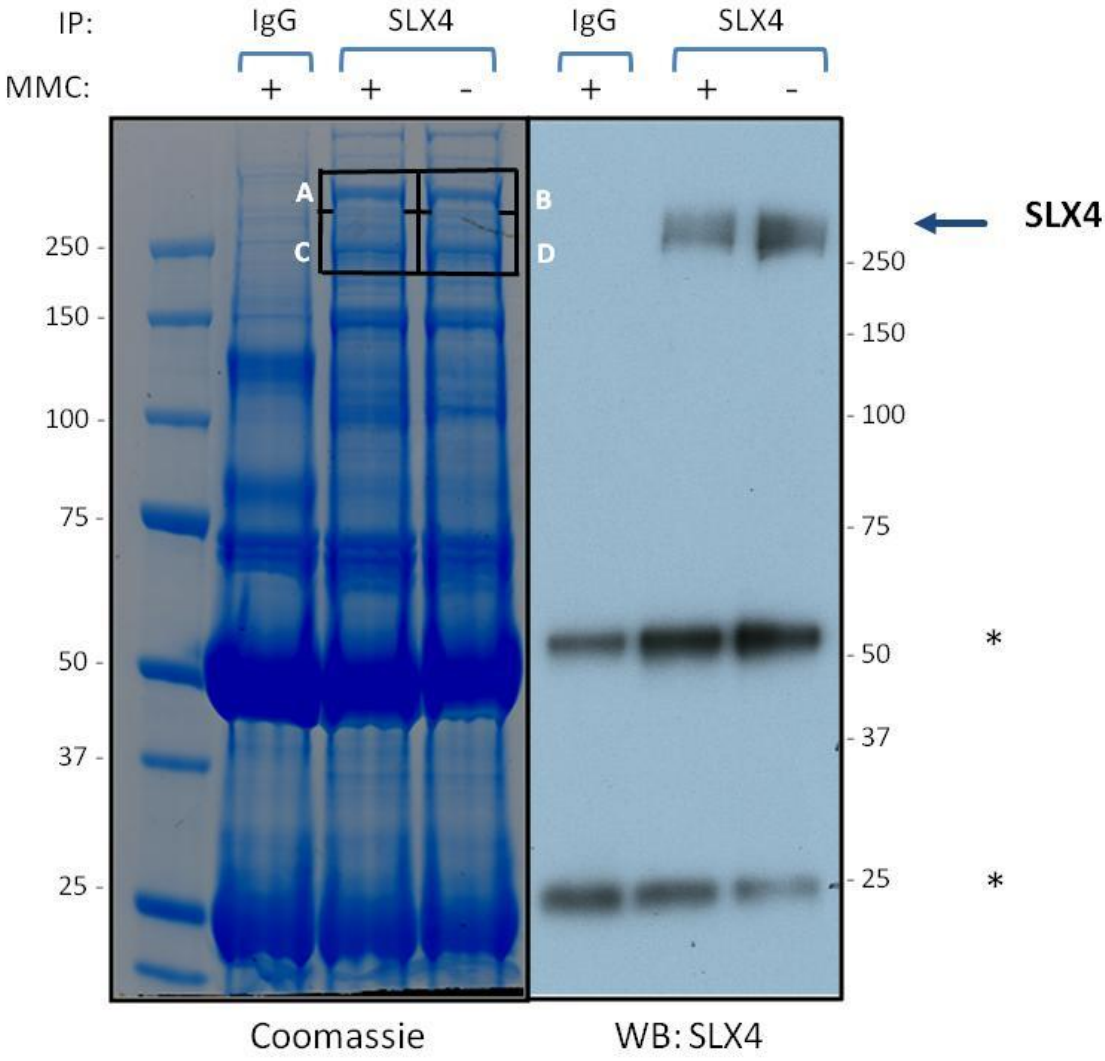

Figure 7: Large scale affinity purification of human SLX4.
HEK293 cells were lysed in buffer containing 300mM NaCl, protease and phosphatase inhibitors. Cell lysates were subjected to immunprecipitation with sheep anti-SLX4 antibodies or sheep anti-GFP antibodies (IgG). Left panel: Coomassie staining. Right panel: western blot using antibodies against SLX4. Bands around 50 kDa and 25 kDa (*) are the heavy and light chain of antibodies respectively.

Peptide	Ratio + MMC / - MMC	Peptide sequence	Residues
1	1.15	SRDCSSQTQISSLR	Ser 1271+Thr 1273
2	1.23	GGTSQVGSPTLLSPAVPSK	Ser 1066
3	1.60	EGSLPHSDDAGDYEQLFSSTQGEISEPS QITSEPEEQSGAVR	Thr 990

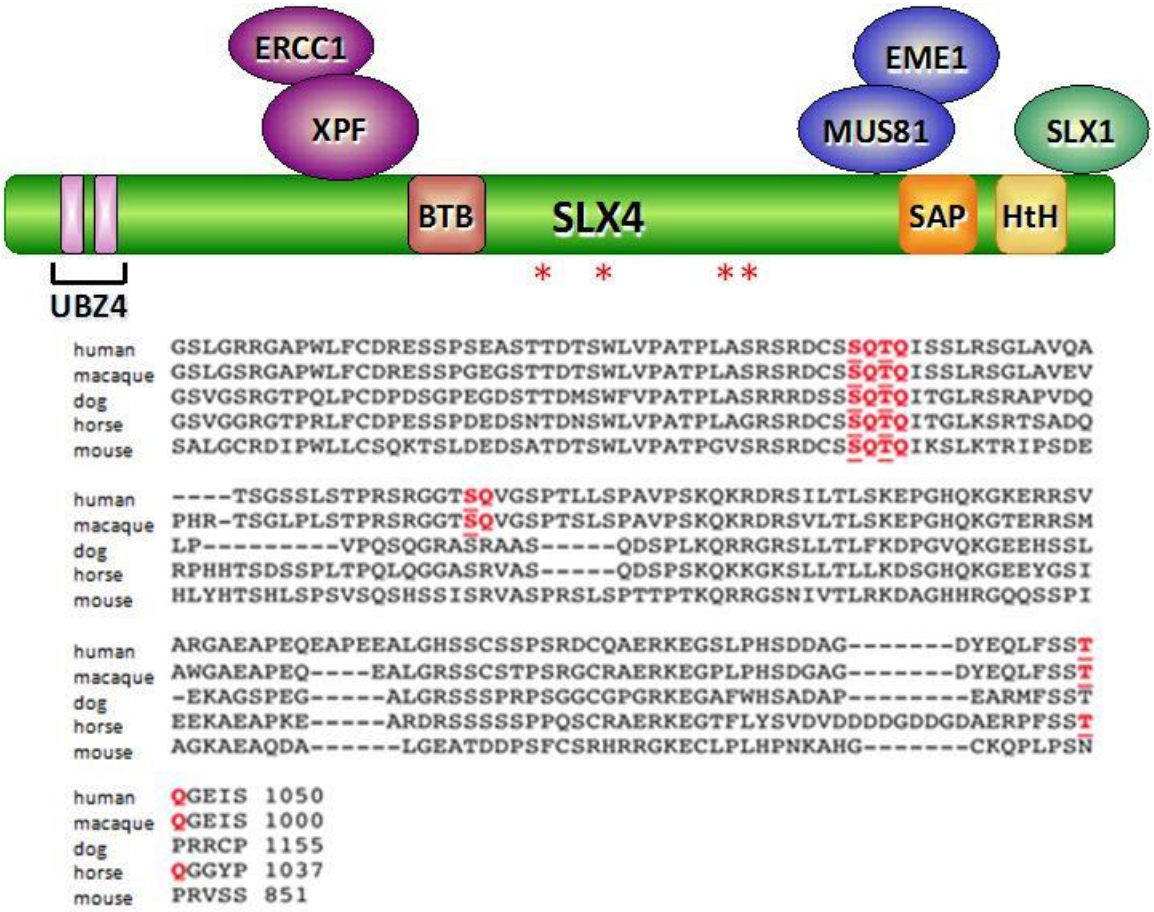

Figure 8: SLX4 phospho-SQ/TQ sites that increase in abundance after MMC treatment.

Upper panel: list of SLX4 peptides found to be phosphorylated on one or more SQ/TQ motifs after MMC treatment. Middle panel: approximate positions of SQ/TQ residues (*) on human SLX4 and sequence alignment showing conserved phospho-SQ/TQ motifs from different species. Lower panel: alignment of region of SLX4 harboring the phospho-SQ/TQ motifs.

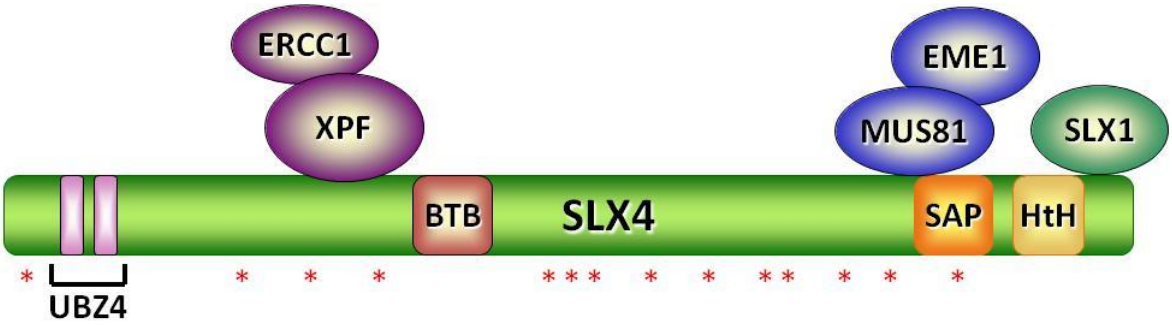

Peptide	Peptide sequence	Residues	Peptide		Peptide sequence	Residues
1	NQQEPSPNLSRE	Ser 169	11	✓	QEPSQSPPRSEA	Ser 1206
2	KKPPVSPPLLLV	Ser 467	12		CDRESSPSEST	Ser 1244
3	LSERRSPALHGT	Ser 584	13		CLTPVSPGTSD	Thr 1326 + Ser1329
4	GSRGPSPSASQ	Ser 601	14	✓	RQGHRSPSRPH	Ser 1342
5	WLEGGSPVSGQL	Ser 884	15		GHPHSSPLAPHP	Ser 1365
6	APWQASPPHPCR	Ser 1028	16		RFLKHSPPGPSF	Ser 1377
7	PPQGGSPRGSHH	Ser 1044	17	✓	PLSTSSPSRRMN	Ser 1453
8	TSQVGSPTLLSP	Ser 1070	18		SRDCRSPGLLDTTP	Ser 1469 + Thr1476
9	SPTLLSPAVPSK	Ser 1075	19		YSIMETPVLKK	Thr 1571
10	KALEISPRSCEL	Ser 1185	20	✓	TPPSRSPTKEAP	Thr 1666 + Ser1681

Figure 9: Identification of putative CDK (SP/TP) residues on SLX4 by phospho-mapping analysis. Upper panel: approximate positions of SP/TP residues on SLX4, showed by red asterisks (*). Lower panel: list of peptides found to be phosphorylated on one or more SP/TP residues. Green check marks indicate peptides with the most stringent consensus sequence for CDKs.

3.2.3 Interaction of SLX4 with MUS81-EME1 is cell-cycle regulated.

In the western blot analysis of the large scale SLX4 immunoprecipites for phospho-mapping shown in **Fig.7**, I also checked the precipitates for known SLX4 interactors including XPF and MUS81. As shown in **Fig.10**, the amount of XPF in SLX4 precipitates was similar before and after treatment of cells with MMC. However, the level of MUS81 was drastically reduced after exposure of cells to MMC. To investigate further, I immunoprecipitated SLX4 from HEK293 cells treated with a range of DNA damaging agents: mitomycin C (MMC), camptothecin (CPT), hydroxyurea (HU) and ionizing radiation (IR). MMC induces intrastrand and interstrand crosslinks, whereas camptothecin inhibits the DNA topoisomerase I and consequently provokes collisions between the replication fork and topoisomerase-I cleavable complexes (Liu, Desai et al. 2000). The ribonucleotide reductase inhibitor HU blocks DNA synthesis by "starving" DNA polymerase at replication forks of dNTPs (Skoog and Bjursell 1974). Finally IR targets DNA by inducing double strand breaks. The interaction between XPF and SLX4 was not affected at any level by any of these treatments (**Fig.11A**). The situation for MUS81 was dramatically different. Exposure of cells to MMC, CPT, HU and even IR reduced the level of MUS81 detected in SLX4 precipitates to the extent that prolonged exposure of films was needed to detect MUS81 (**Fig.11A**). The levels of MUS81 in cell extracts was largely unaffected by the genotoxic insults (**Fig.11B**).

There are two main possibilities to explain dissociation of MUS81 from SLX4 after treatment of cells with genotoxins. DNA damage-induced signaling may induce dissociation of the two proteins, by ATM/ATR-dependent phosphorylation of either protein, for example. Alternatively it may be that the interaction of MUS81 and SLX4 is cell cycle regulated, and the genotoxins are simply arresting cells at a stage where SLX4

interacts less well with MUS81. To distinguish between these possibilities I separated cells according to cell cycle stage by counterflow centrifugal elutriation (CCE), a technique that does not rely on drugs to synchronize cells. The key principle of CCE is that cells at different cell cycle stages have different sizes; more precisely, cells in G1 stage (2n DNA content) are smaller than to cells in S phase which are in turn smaller than cells in G2 phase . Cells are centrifuged in a special rotor and smaller cells (G1) sediment first, followed by cells in S and G2 phase. As shown in **Fig.12A**, I collected fractions, corresponding to cells in G1, S, and G2 phase which were first stained with propidium iodide and subjected to FACS analysis to check DNA content which is a readout of cell cycle stage. Extracts from the different fractions were subjected to immunoprecipitation with antibodies against SLX4. Western blotting of precipitates revealed that binding of XPF with SLX4 was constant throughout the cell cycle (**Fig.12B**), whereas the interaction between SLX4 and MUS81 was almost completely absent during G1 and early S phase (fractions F1-F3) but became apparent towards the end of S-phase and beginning of G2 phase (fractions F4-F6). Taken together these experiments strongly suggest that the interaction of SLX4 and MUS81-EME1 is regulated in a cell cycle-dependent manner.

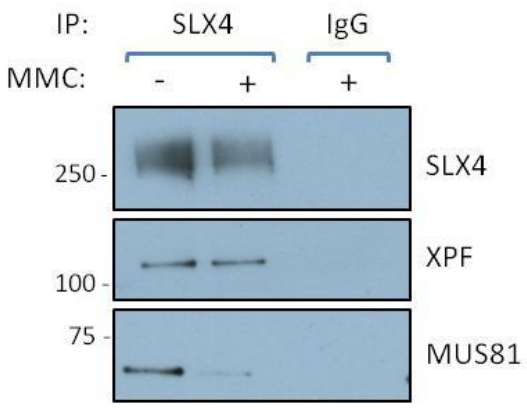

Figure 10: SLX4-MUS81 is reduced in cells exposed to MMC.

Large scale SLX4 immunoprecipitates, as described in Fig. 3, were subjected to western blot analysis with the antibodies indicated. IgG: sheep anti-GFP (negative control).

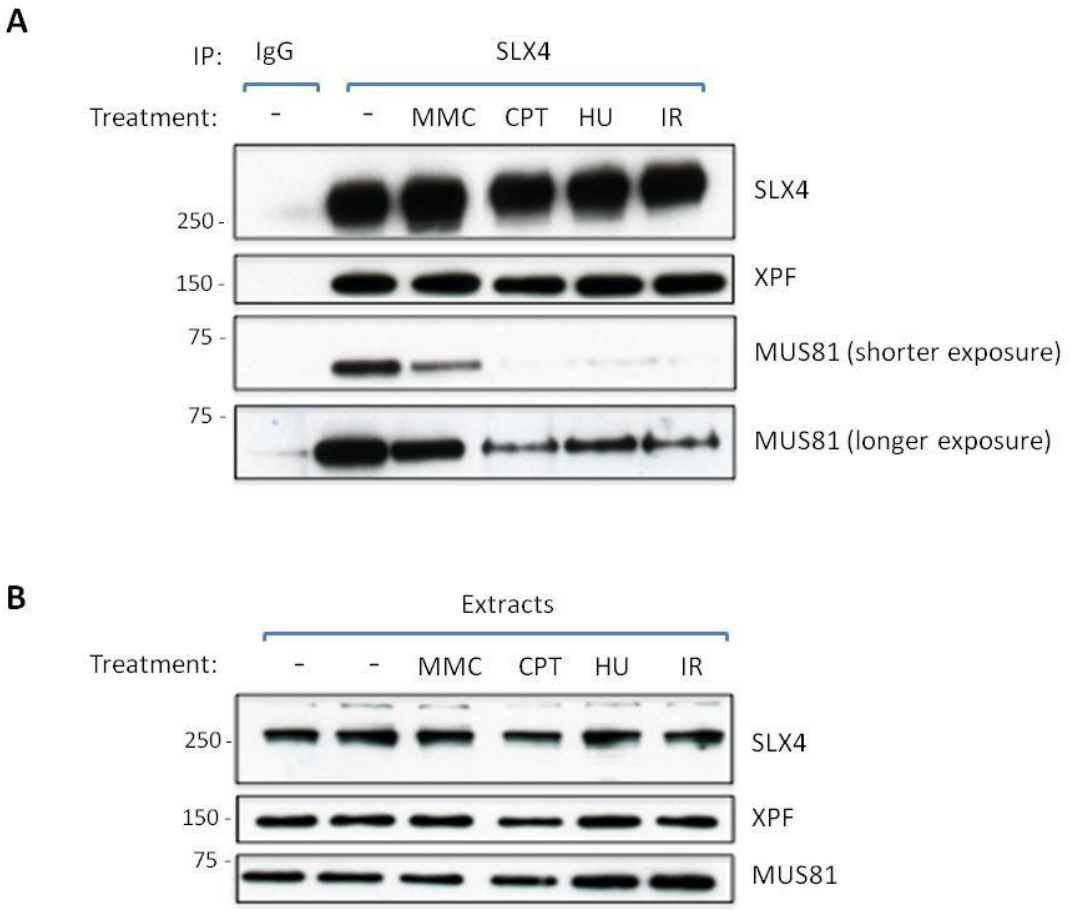

Figure 11: SLX4-MUS81 interaction is affected by different genotoxins.

HEK293 cells were treated with mitomycin C (MMC; 200ng/ml), camptothecin (CPT; 2µg/ml), hydroxyurea (HU; 2mM), or Ionizing Radiation (IR; 10 Gy). Cells were lysed and SLX4 immunoprecipitates were analyzed by western blotting with the antibodies indicated (A). Expression of proteins in whole cell extracts was examined by western blotting (B).

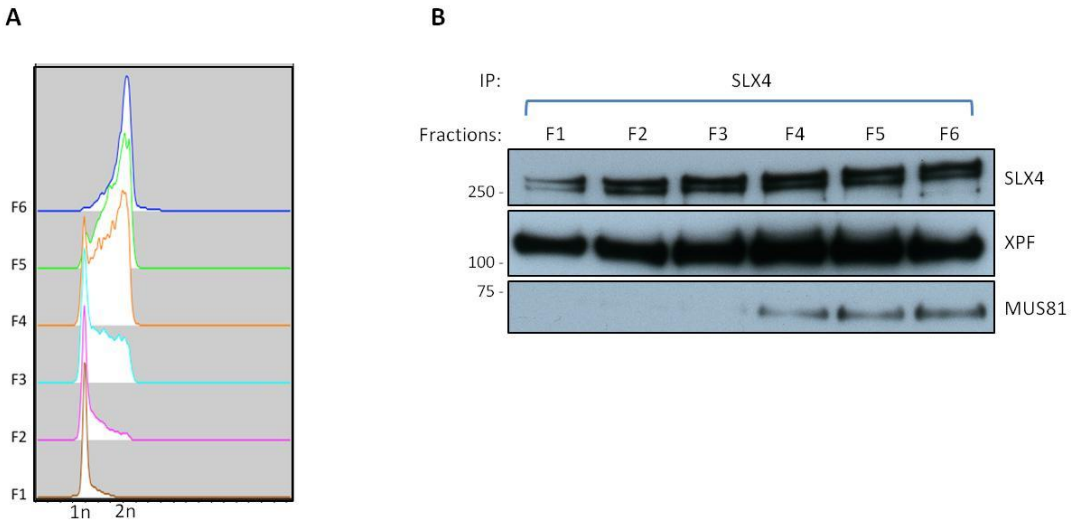

Figure 12: SLX4-MUS81 interaction is regulated throughout the cell cycle.

Cells were fractionated according to size by counterflow centrifugal elutriation (CCE) resulting in 6 fractions. For each sample the DNA content was measured by flow cytometry (A). Samples were then lysed and anti-SLX4 precipitates were subjected to western blotting with the antibodies indicated (B).

3.3 DISCUSSION AND FUTURE WORK

In this chapter, I described the identification of *in vivo* sites of phosphorylation on human SLX4.

SLX4 appears to be phosphorylated in response to DNA damage on at least three ATM/ATR-consensus sites (SQ/TQ motifs) (**Fig.8**). It is perhaps surprising that I only identified three sites of SQ/TQ phosphorylation in human SLX4 given that at least six SQ/TQ sites were identified in yeast Slx4 (Flott et al., 2007). None of the three SQ/TQ phospho-sites identified in human SLX4 are located in any of the known functional domains in SLX4**.** However, of these sites, Thr1273 was previously found by another team in a global analysis (Mu et al. 2007) and I noticed that this residue is conserved in many SLX4 orthologues, suggesting that it is of functional importance. Thr1273 does not reside in any of the known modular SLX4 domains, and so it is difficult to predict functional consequences. However it is possible that the three dimensional folding of SLX4 might bring Thr1273 in close proximity with SLX4 interacting proteins. In the meantime phospho-specific antibodies have been raised against the sites identified in this study and these are currently being tested.

It is possible that under the conditions I used in my experiments I missed some phospho-sites, for example because the relevant tryptic peptides are too large. It might also be that the phospho-forms of SLX4 bind very tightly to chromatin and are not made soluble by my lysis conditions, in this regard I could use a denaturant in the lysis buffer which could be dialysed away before immunoprecipitation. It would be interesting to treat cells with another cross-linking agent that induces only inter-strand crosslinks like SGJ-136 (Pepper, Hambly et al. 2004), as most the lesions induced by

MMC are mono-adducts. As future work, I would also like to scale up even further, and to use proteases other than trypsin. Testing the ability of SLX4 bearing mutations in the phospho-sites I identified to rescue the defects in $SLX4^{-/-}$ MEFs would also be relevant to understand the function of this posttranslational modification.

Although I only identified three phospho-SQ/TQ motifs, I found a relatively large number of SP/TP sites in SLX4. These could be targeted by proline-directed protein kinases such as MAP kinases, DYRK isoforms, for example or CDKs. It will be important to raise antibodies against these sites and to study the cell cycle dependence. In this regard, antibodies have been raised against one of the residues identified in my experiment: Ser1453 (**Fig.9**, peptide 17), because it is interesting for several reasons. Previous work carried out in this laboratory identified a physical interaction between PLK1 and SLX4. PLK1 belongs to the Polo-like kinase family that plays essential roles in different stages of mitosis and cytokinesis, including the regulation of centrosome maturation and spindle assembly (Donaldson, Tavares et al. 2001). PLK1 has a polo box that binds to subsets of phospho-SP/TP sites and the consensus polo box binding motif for PLK1 is S-pS/pT-P. In this light, SLX4 has four residues that look like polo box binding sites, and one of these is Ser1453. When this residue is mutated to Ala, the interaction between SLX4 and PLK1 is abolished (data not shown), so it appears that CDK phosphorylation of SLX4 creates a docking site for PLK1. Future studies could be carried out to investigate the functional significance of this phosphorylation. An article recently published by Steve West's laboratory, showed that SLX4-MUS81 association increases in S/G2 and that the interaction is dependent on CDKs and PLK1 activity but the mechanisms and consequences for DNA repair are unclear. After treating cells with genotoxins such as MMC, CPT, and HU, my data showed a reduction of MUS81 levels in SLX4 immunoprecipitates. It is known that these drugs create DNA damages as

well as arresting cells during S phase. However, cell-cycle experiments by using the CCE technique that does not create any DNA damage in cells, showed that MUS81-SLX4 interaction was more prominent during late S, G2 phase. It is possible that the dynamism in the MUS81-SLX4 binding is due to a combination of cell cycle progression and an active disruption of the interaction. As future goal it will be important to investigate this hypothesis by analyzing the FACS profile of cells treated with MMC, HU and CPT to check at which cell cycle stage they arrest. Finally, in the future it would be interesting to see which residues are implicated in the SLX4-MUS81 interaction, whether they are all CDKs substrates or the binding is also affected by the phosphorylation mediated by ATM/ATR, and analyze whether MUS81 post-translational modifications also contribute to enhancing the interaction.

4 IDENTIFICATION OF NOVEL SLX4-INTERACTING PROTEINS

4.1 INTRODUCTION

Our lab previously carried out a large-scale SLX4 purification from HEK293 cells overexpressing GFP-tagged SLX4. This resulted in the identification of three different endonucleases (XPF/ERCC1, MUS81/EME1, SLX1), TRF2-RAP1, MSH2-MSH3, PLK1 and C20orf94 (Muñoz et al. 2009). However, this approach can mask weaker interactions and overexpression can titrate out low abundance interactors. Since I had immunoprecipitated endogenous SLX4 for phospho-mapping, I decided to use the gel from the same experiment to identify new SLX4-interacting proteins.

4.2 RESULTS

4.2.1 Mass spectrometric identification of proteins interacting with endogenous SLX4: SCF complex

Fig.7 shows the gel on which I ran large scale anti-SLX4 immunoprecipitates. I subsequently cut each lane into slices which were subjected to tryptic digest and the resulting peptides were analysed by mass fingerprinting. This experiment revealed most of the known SLX4-interacting proteins, but I also identified two components of the canonical SCF complex: FBXO11 and CUL1. (**Table 4**) SCF is a multisubunit protein ligase (E3) that belongs to a family of Cullin-RING ligases (CRLS). The canonical SCF is composed of an enzymatic core that contains CUL1 and the RING protein RBX1. At the N-terminal CUL1 binds to its adaptor protein SKP1, the latter interacts with an F-box family member (in this case FBXO11) that confers substrate specificity (Petroski and Deshaies 2005).

Gene symbol	Score (-MMC)	Score (+MMC)	Peptides matched (-MMC)	Peptides matched (+MMC)	Coverage (-MMC)	Coverage (+MMC)
AHNAK	12003	7160	597	391	47%	31%
SLX4	396	301	32	14	11%	4%
EPPK1	3793	4381	158	175	18%	18%
PRRC2C	1911	761	143	72	31%	18%
UBR4	1473	1264	88	64	14%	10%
ALMS1	1247	795	102	73	24%	20%
MYCBP2	711	1019	44	59	9%	11%
SLX4	603	323	29	16	13%	6%
HERC2	355	/	29	/	5%	/
PRRC2C	/	761	/	72	/	18%
PRRC2C	8252	8292	534	519	53%	54%
MAP1B	3101	1905	134	84	39%	31%
RANBP2	2363	1918	108	94	25%	22%
UBR5	4047	4870	165	173	36%	42%
PRRC2B	2473	2667	106	123	36%	42%
PHF3	2264	2300	142	131	39%	40%
PRRC2C	2222	2667	165	190	39%	41%
SEC16A	1708	1811	86	82	35%	36%
SLX4	1343	1142	55	60	20%	23%
SLX4	7287	6386	326	277	46%	38%
PRRC2C	3029	3016	245	299	39%	41%
SLX4	3240	1913	136	93	34%	32%
NUP153	2486	2482	110	118	46%	52%
PRRC2C	1218	923	104	88	27%	25%
BMP2K	2881	2424	122	111	47%	46%
DHX8	1643	902	81	52	39%	34%
SLX4	540	562	32	27	13%	13%
ERCC4 (XPF)	5435	4349	187	156	67%	62%
FBXO11	1096	914	48	46	37%	40%
CUL1	633	378	32	15	35%	17%
MUS81	238	/	10	/	17%	/
EME1	135	/	6	/	9%	/
PLK1	59	/	3	/	6%	/
ERCC1	2081	1129	77	48	82%	44%
SLX1A	808	326	38	20	55%	31%

Table 4: Proteins interacting with endogenous SLX4 in HEK293 cells identified by mass fingerprinting. Lysates from anti-SLX4 immunoprecipitates have been run on a SDS-PAGE gel and the gel has been stained with Colloidal Coomassie Blue. Each lane has been cut into slices, digested with trypsin and the resulting peptides analysed by mass fingerprinting. Proteins found in the same lane have been grouped together in the table. Proteins found in more than one lane, appear multiple times in the corresponding groups.

I first wished to confirm these interactions. HEK293 were lysed in a buffer containing protease, phosphatase and deubiquitinase inhibitors (iodoacetamide), then SLX4 was immunoprecipitated from the extract using anti-SLX4 antibodies and western blotting against FBXO11 and CUL1 was performed. The analysis confirmed both interactions, as I found bands at the expected molecular weight: around 103kDa for FBXO11 and around 89kDa for CUL1 (**Fig.13**). The other two components of the SCF complex (SKP1 and RBX1) did not appear in the mass spectrometric analysis, but nonetheless RBX1, but not the SKP1 adaptor protein, was detected when SLX4 precipitates were probed with the relevant antibodies (**Fig.13**).

Cullins need to be NEDDylated to be active (Saha and Deshaies 2008). NEDD8 is a small protein that is more than 50% identical to ubiquitin. Protein neddylation requires the action of an E1 NEDD8 Activating Enzyme (NAE) and an E2 NEDD8 Conjugating Enzyme (Gong and Yeh 1999). In the SCF complex, NEDD8 is reversibly conjugated to a conserved Lys that resides in close proximity to the RING-binding region of CUL1 (Wu, Chen et al. 2000). It has been reported that the covalent attachment of NEDD8 enhances CUL1-dependent ubiquitin-ligase activity *in vitro* (Ohh, Kim et al. 2002). When cells are treated with MLN4924, the molecule binds to and inhibits the NAE, therefore it compromises the ubiquitination of SCF-target substrates (**Fig.14**). I hypothesized the interaction of CUL1 with SLX4 might control SLX4 complex stability and to verify this I tested the effect of treating cells with MLN4924, an inhibitor of the NEDD8 activating enzyme (Soucy, Smith et al. 2009). Cells were exposed to MLN4924 for 6 hours before lysis, and extracts were subjected to SLX4 immunoprecipitation. As shown in **Fig.15A**, exposure of cells to MLN4924 resulted in an increase in CUL1 electrophoretic mobility which others have shown to reflect CUL1 de-neddylation

(Lee, Sweredoski et al. 2011; Zhao, Xiong et al. 2012). However the stability of SLX4 or the associated endonucleases was unaffected (**Fig.15B**).

4.2.2 SLX4 interacts with the E3 ubiquitin ligase UBR5

UBR5, an E3 ubiquitin-protein ligase which is a component of the N-end rule pathway ((Varshavsky 2011), was also detected by mass fingerprinting of SLX4 immunoprecipitates. UBR5 recognizes and binds to proteins bearing particular N-terminal residues, leading to their ubiquitination and subsequent degradation. UBR5 has also been shown to regulate DNA damage responses by controlling RNF168 stability (Gudjonsson, Altmeyer et al. 2012). I confirmed the interaction of SLX4 with UBR5 by western blotting. In SLX4 immunoprecipitates, I detected a band of the expected molecular weight for UBR5 (**Fig.16A**); however, in UBR5 immunoprecipitates I found only one of the most slowly migrating SLX4 bands (**Fig.16A,** asterisk). This was an intriguing observation, as SLX4 always exists as a series of bands on SDS-PAGE; the nature of these different species is not clear but they could represent post-translationally modified forms of SLX4.

I wished to further verify the SLX4-UBR5 interaction. In this light, UBR5 was depleted from HEK293 cells using three separate siRNAs. As shown in **Fig.16B**, western blotting cell extracts showed that these siRNA species cause a major reduction in UBR5 expression. I found that siRNA 1 abolished the UBR5 band in SLX4 precipitates (**Fig.16C**).

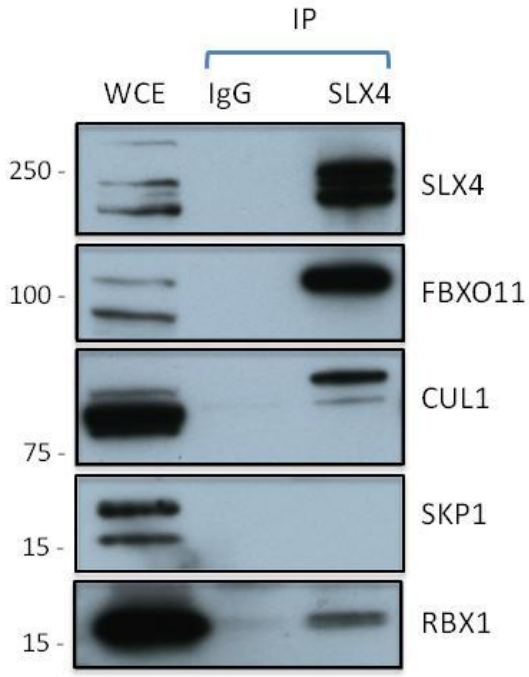

Figure 13: SLX4 interacts with components of the SCF^{FBXO11} complex.

HEK293 cells were lysed and subjected to SLX4 immunoprecipitation. Precipitates were subjected to western blot analysis with the antibodies indicated.

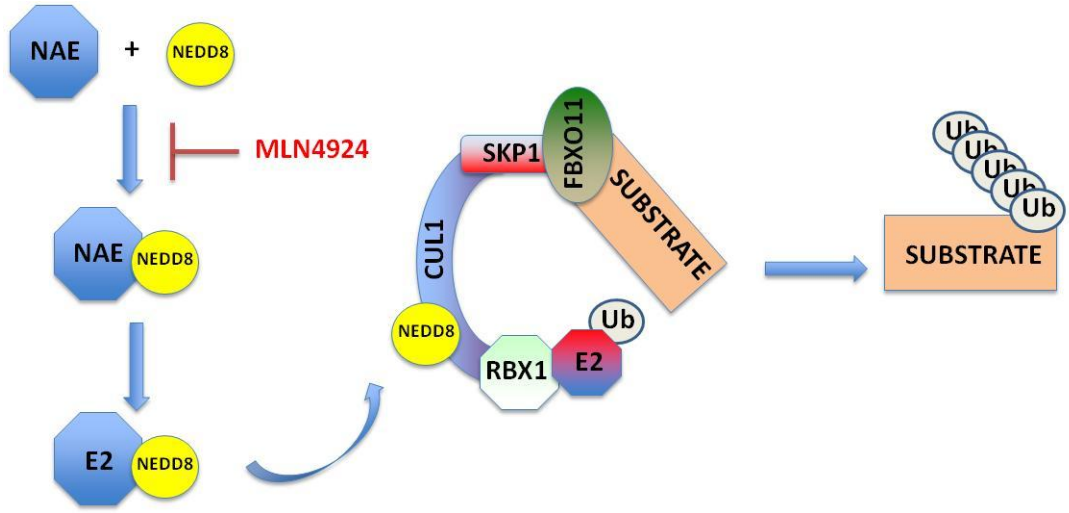

Figure 14: Schematic view of MLN4924 inhibition.

The SCF complex promotes the poly-ubiquitination of target substrates leading to their degradation. The conjugation of the ubiquitin-like protein NEDD8 to CUL1 (neddylation), stimulates the ubiquitin transfer from SCF-bound E2 to the substrate lysine and the polymerization of the ubiquitin chain. Neddylation is a three steps pathway, where in the first step NEDD8 binds to the E1 NEDD8-activting enzyme (NAE). The competitive inhibitor, MLN4924 disrupts the interaction between NEDD8 and NAE, therefore blocks the neddylation of the SCF complex and prevents the ubiquitination of SCF substrates.

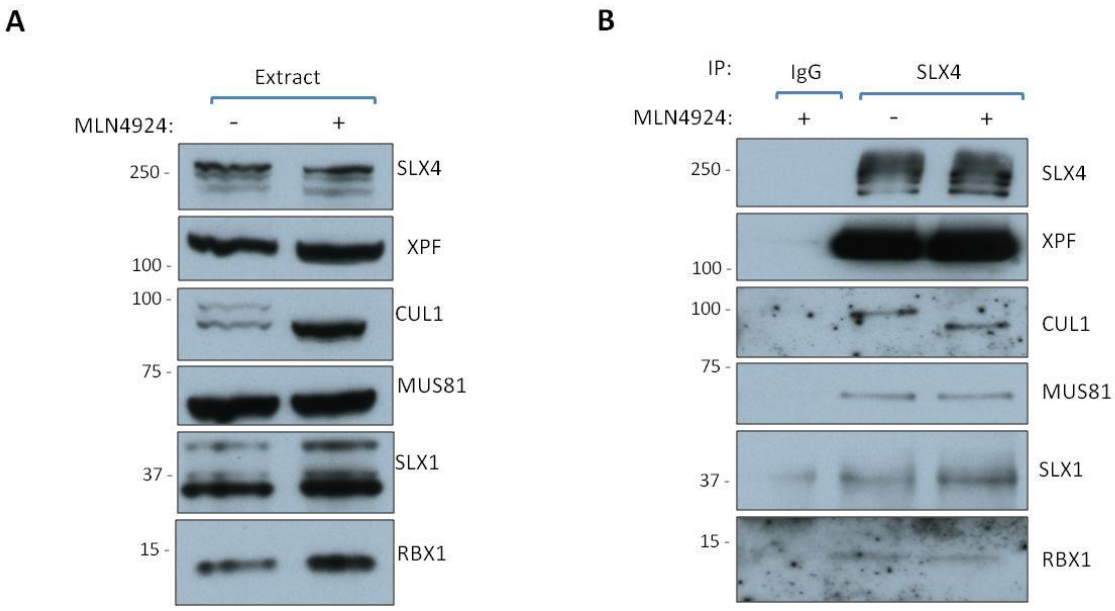

Figure 15: MLN4924 does not affect the interaction of SLX4 with XPF, MUS81 or SLX1.

HEK293 cells were treated, or not with MLN4924 (3µM; 6 hr). The expression levels of the indicated proteins were analyzed in whole cell extracts by western blotting (A). Extracts were subjected to SLX4 immunoprecipitation and precipitates were subjected to western blotting with the indicated antibodies (B).

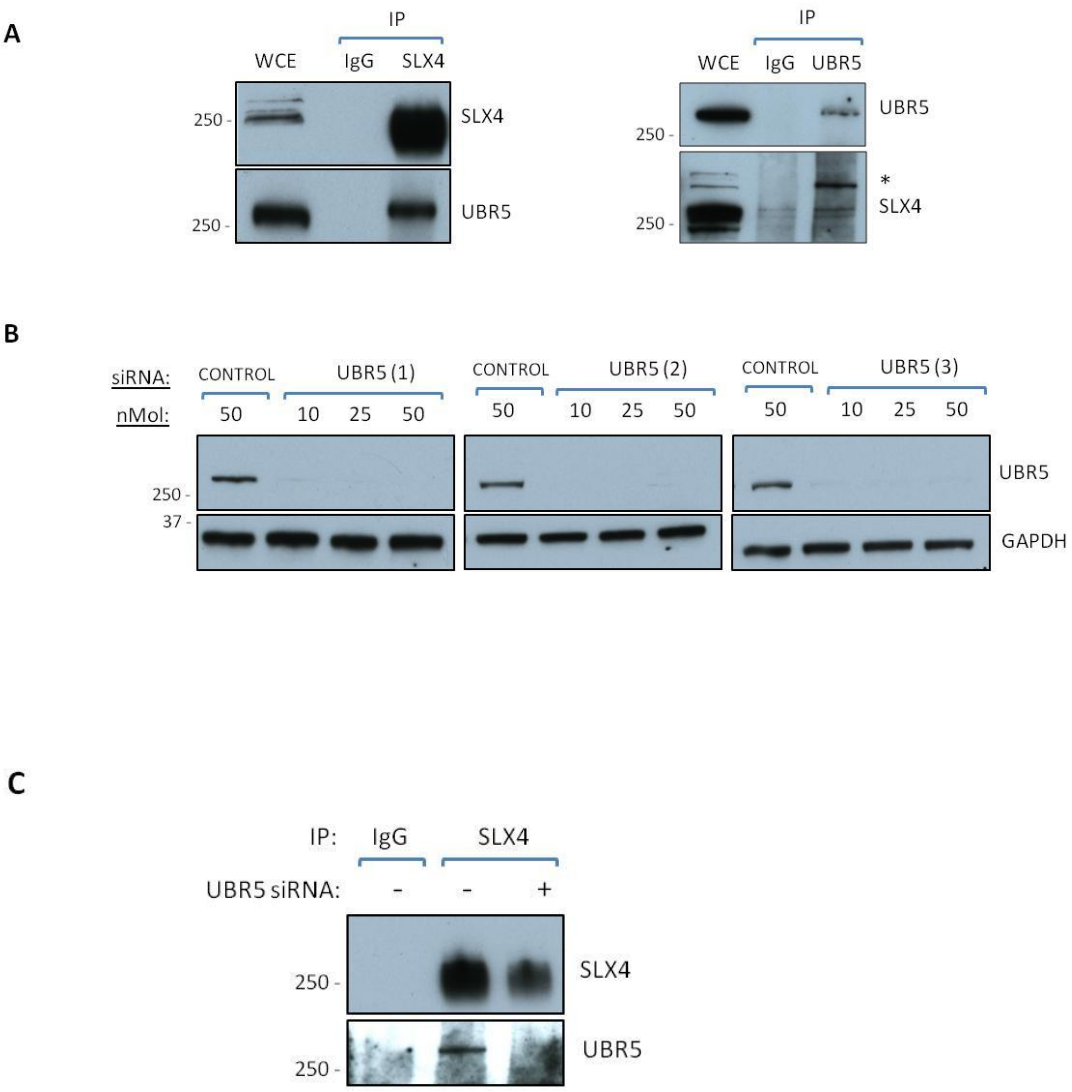

Figure 16: SLX4 interacts with the UBR5 E3 ubiquitin ligase

(A) HEK293 extracts were subjected to immunoprecipitation with either anti-SLX4 or anti-UBR5 antibodies and western blot analysis with indicated antibodies was performed. Asterisk indicates the SLX4 slow migrating band. (B) Cells were transfected with three separate UBR5 siRNAs (10, 25 or 50 nM) or with a control (scramble siRNA 50 nM). (C) Cells were transfected with UBR5 siRNA number 1 (10 nM), and SLX4 was immunoprecipitated from UBR5-depleted extracts and western blotting analysis of the indicated proteins was performed.

4.3 DISCUSSION AND FUTURE WORK

In this chapter I identified two E3 ligases in SLX4 immunoprecipitates: UBR5 and SCF^{FBXO11} and confirmed the interactions by western blotting. It is still unknown whether SLX4 directly binds to these ubiquitin ligases or whether the interaction is through one of the SLX4-binding partners. Although the meaning of these interactions is still a conundrum, some hypothesis can be made, based on the literature.

Regarding UBR5, it has been reported an involvement in the DNA damage response, by targeting RNF8 and RNF168 for proteasomal degradation (Gudjonsson et al. 2012). RNF8 and RNF168 are two E3 RING ligases that are recruited to the chromatin after double strand breaks. They modify the histone variant H2A and H2AX by adding K63 linked chains, which induce the recruitment of downstream effectors leading to the repair of the DNA damage (Bartocci and Denchi 2013). UBR5 controls an excessive spreading of ubiquitinated chromatin at damaged chromosomes, by contributing to the degradation of RNF8 and RNF168. A recent study revealed that the shelterin component TRF2 is involved in preventing the DNA damage response at telomeres, by blocking the signaling cascade at the level of RNF168 (Okamoto, Bartocci et al. 2013). Interestingly the same team found UBR5 in TRF2 immunoprecipitates. Given that TRF2 is one of the components of the SXL4 scaffold and that SLX4 localizes on telomeres (Svedsen et al. 2009; Wilson et al. 2013), it is possible that the SLX4-UBR5 interaction is mediated by TRF2. It would be interesting to see whether the SLX4-UBR5 interaction is compromised in TRF2 depleted cells.

UBR5 could also directly bind and modify SLX4. Western blot analysis of UBR5 immunoprecipitates using antibodies against SLX4, showed that only a slow migrating form of SLX4 binds to the ligase and it would be interesting to test whether this corresponds to an ubiquitinated form of SLX4, by treating samples with non-specific deubiquitinases.

Regarding SCF^{FBXO11}, it is part of a family of Cullin-RING ligases (CRLs). Human cells express seven different cullins and each of them nucleates different multisubunit complexes. CUL1-based E3 ligases are called SCF ubiquitin ligases. The canonical SCF is composed of CUL1, the adaptor protein SKP1, the RING containing protein RBX1, and the F-BOX protein that confers substrate specificity and varies depending on the target substrate (**Fig.14**). Preliminary experiments showed that SLX4 interacts with FBXO11, RBX1, and CUL1. Interestingly the fraction of CUL1 that co-immunoprecipitates with SLX4 is neddylated, which suggests that the SCF^{FBXO11} complex binds to the scaffold as an active E3 ligases. Suprisingly, SLX4 did not interact with the adaptor SKP1. It is known that another cullin, CUL3, which is part of the CRL3 (Culling-RING ligase 3) uses as adaptor BTB-domain containing proteins (Petroski et al., 2005) and SLX4 contains a BTB domain. Moreover the mass spectrometric analysis of SLX4 immunoprecipitates did not find any peptide corresponding to CUL3, so it could be possible that not only CUL3, but also CUL1 binds to BTB-proteins and that SKP1 is not the only adaptor for CUL1. If the same assembly of the complex was present in mouse cells, it would be interesting to analyze the CUL1-FBXO11 interaction in $Slx4^{-/-}$ cells.

As for UBR5, SCF could also be involved in the binding of other SLX4 component or the

interaction could be mediated through a still unknown ubiquitinated protein that binds to the UBZ4 domains of SLX4. An extensive screening of all the SLX4 partners should be performed to address this question.

5 DOES SLX4 INTERACT WITH MSH2-MSH3?

5.1 INTRODUCTION

MSH2-MSH3 is a heterodimer which functions by recognizing insertion/deletion loops in the mismatch repair, gene conversion, or single strand annealing pathways. Although MSH2-MSH3 was detected in mass fingerprinting analysis of precipitates of tagged and overexpressed human SLX4 (Svendsen et al. 2009), the mass fingerprinting analysis described in section 3, didn't detect neither MSH2 nor MSH3 in SLX4 precipitates. Although this might be due to the stringent conditions used for the immunoprecipitation (300mM NaCl), it might be that the reported interaction of SLX4 with MSH2-MSH3 is an artifact of overexpression. I decided to test if endogenous SLX4 interacts with MSH2-MSH3.

5.2 RESULTS

5.2.1 Analysis of SLX4-MSH2/3 interaction

Western blotting of anti-SLX4 immunoprecipitates revealed the presence of both MSH2 and MSH3 (**Fig.17**). In order to discriminate which subunit of the MSH2-MSH3 complex interacts with SLX4, I used a yeast two hybrid assay. This method has advantages over other biochemical approaches. It assays protein-protein direct interactions, it requires only the cDNA of the gene of interest in contrast to high quantity of cell lysate and good quality of antibodies for immunoprecipitation experiments. Moreover weak and transient interactions are detected and amplified. However, one of the disadvantages is that this system makes use of *S. cerevisiae* as a host; for this reason, a yeast protein could bridge the interaction between proteins of interested. As shown in **Fig.18**, the yeast-two-hybrid experiment revealed that MSH2, and not MSH3 interacts with SLX4. I next used different SLX4 deletion fragments to

map the SLX4 region binding to MSH2. This revealed that the X4 peptide of SLX4 (residues: 1-792) interacts with MSH2 (**Fig.19**). Surprisingly, MSH2 didn't interact with any of the fragments (X1, X2, X3) that narrow this region down further.

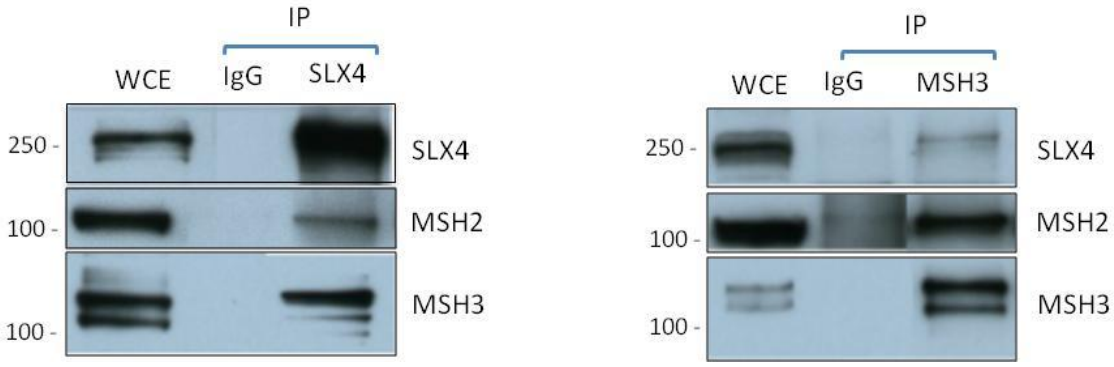

Figure 17: SLX4 interacts with the MSH2/MSH3 complex.

HEK293 extracts were subjected to immunoprecipitation with either anti-SLX4 or anti-MSH3 antibodies and western blotting analysis was performed with the indicated antibodies.

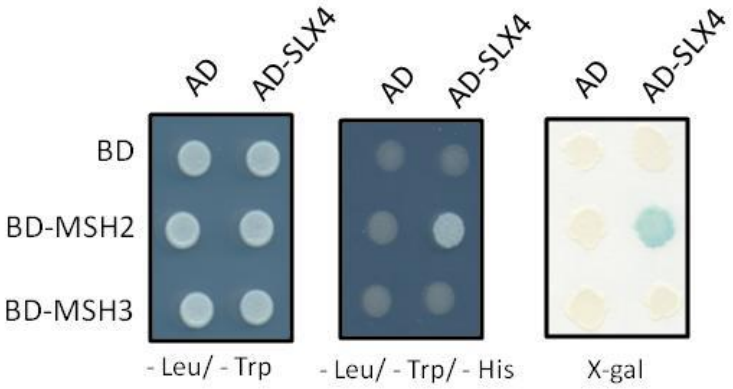

Figure 18: Yeast two hybrid assay shows that SLX4 directly interacts with MSH2.

SLX4 was cloned into activation domain vector (AD) and MSH2 or MSH3 into GAL4 DNA-binding domain vector (BD). To select both vectors, cells were grown on selective medium lacking LEU and TRP. Cells were then replica plated to medium lacking LEU, TRP, and HIS, to test for activation of *HIS3* reporter gene, and then replica plated on x-gal membrane to test for LacZ reporter gene activity.

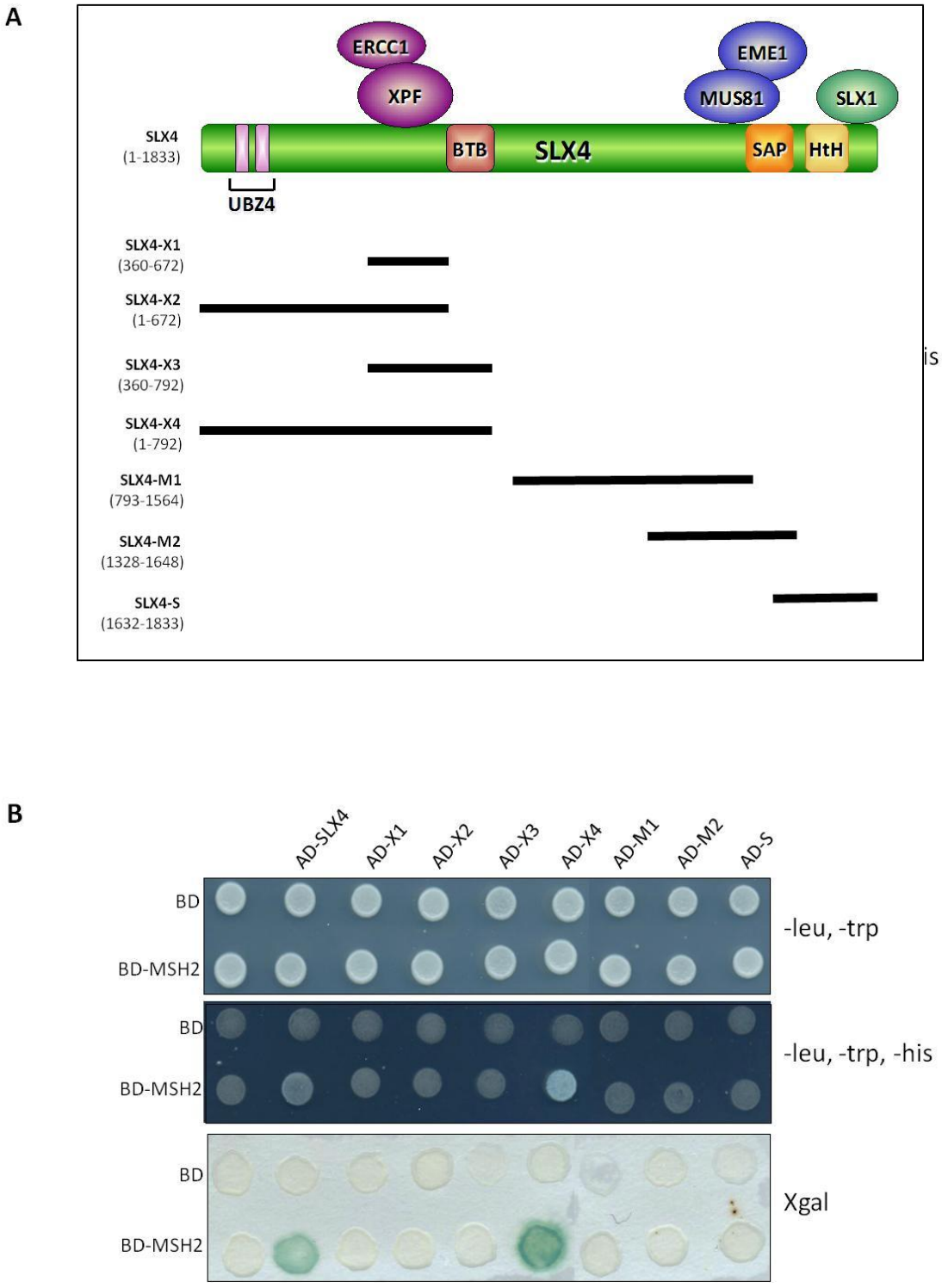

Figure 19: Yeast two hybrid assay with MSH2 and SLX4 deletion SLX4 fragments.

A: schematic view of the SLX4 sequence and positions of the different fragments.
B: yeast two hybrid analysis between MSH2 and different SLX4 fragments.

5.3 DISCUSSION AND FUTURE WORK

In this section I confirmed by yeast-two-hybrid assay that SLX4 interacts with the MSH2-MSH3 complex through MSH2. I also found that the N-terminal region of SLX4 is involved in the binding, but none of the SLX4 truncation constructs that narrow this region down further interacted with MSH2. There are several possibilities that could explain this result. It is possible that the SLX4 fragments are not expressed in yeast or that they are misfolded. However it could be that MSH2 might contact multiple points in SLX4. The BTB domain of SLX4 mediates homodimerization and it might be that the MSH2 binding site on SLX4 is only formed after SLX4 dimerizes. This would be more complicated than the interaction between SLX4 and its other components (SLX1, XPF, and MUS81 for example) where small interacting regions could be defined and single point mutations are capable of abolishing binding.

In yeast *S. cerevisiae*, Msh2-Msh3 helps the nuclease activity of Rad1-Rad10 (XPF-ERCC1) during gene conversion and single strand annealing. Although in human it has not been reported an involvement of SLX4 in SSA, it could be possible that SLX4 plays a role in this pathway, given that SLX4 binds both to MSH2-MSH3 and XPF-ERCC1. If I could identify mutations that abolish binding of SLX4 to MSH2, in the future I could carry out rescue experiments to test the effect of SLX4-MSH2/3 interaction on ICL repair and single-strand annealing.

REFERENCES

Akkari, Y. M., R. L. Bateman, et al. (2000). "DNA replication is required To elicit cellular responses to psoralen-induced DNA interstrand cross-links." Molecular and cellular biology **20**(21): 8283-8289.

Al-Minawi, A. Z., N. Saleh-Gohari, et al. (2008). "The ERCC1/XPF endonuclease is required for efficient single-strand annealing and gene conversion in mammalian cells." Nucleic acids research **36**(1): 1-9.

Alpi, A. F. and K. J. Patel (2009). "Monoubiquitylation in the Fanconi anemia DNA damage response pathway." DNA repair **8**(4): 430-435.

Aravind, L. and E. V. Koonin (2001). "Prokaryotic homologs of the eukaryotic DNA-end-binding protein Ku, novel domains in the Ku protein and prediction of a prokaryotic double-strand break repair system." Genome research **11**(8): 1365-1374.

Auerbach, A. D. (1988). "A test for Fanconi's anemia." Blood **72**(1): 366-367.

Bartocci, C. and E. L. Denchi (2013). "Put a RING on it: regulation and inhibition of RNF8 and RNF168 RING finger E3 ligases at DNA damage sites." Frontiers in genetics **4**: 128.

Bergstralh, D. T. and J. Sekelsky (2008). "Interstrand crosslink repair: can XPF-ERCC1 be let off the hook?" Trends in genetics : TIG **24**(2): 70-76.

Bertrand, P., D. X. Tishkoff, et al. (1998). "Physical interaction between components of DNA mismatch repair and nucleotide excision repair." Proceedings of the National Academy of Sciences of the United States of America **95**(24): 14278-14283.

Bhagwat, N., A. L. Olsen, et al. (2009). "XPF-ERCC1 participates in the Fanconi anemia pathway of cross-link repair." Molecular and cellular biology **29**(24): 6427-6437.

Bogliolo, M., B. Schuster, et al. (2013). "Mutations in ERCC4, encoding the DNA-repair endonuclease XPF, cause Fanconi anemia." American journal of human genetics **92**(5): 800-806.

Castor, D., N. Nair, et al. (2013). "Cooperative control of holliday junction resolution and DNA repair by the SLX1 and MUS81-EME1 nucleases." Molecular cell **52**(2): 221-233.

Chaganti, R. S., S. Schonberg, et al. (1974). "A manyfold increase in sister chromatid exchanges in Bloom's syndrome lymphocytes." Proceedings of the National Academy of Sciences of the United States of America 71(11): 4508-4512.

Chen, X. B., R. Melchionna, et al. (2001). "Human Mus81-associated endonuclease cleaves Holliday junctions in vitro." Molecular cell **8**(5): 1117-1127.

Ciccia, A., A. Constantinou, et al. (2003). "Identification and characterization of the human mus81-eme1 endonuclease." The Journal of biological chemistry **278**(27): 25172-25178.

Ciccia, A., C. Ling, et al. (2007). "Identification of FAAP24, a Fanconi anemia core complex protein that interacts with FANCM." Molecular cell **25**(3): 331-343.

Ciccia, A., N. McDonald, et al. (2008). "Structural and functional relationships of the XPF/MUS81 family of proteins." Annual review of biochemistry **77**: 259-287.

Cimprich, K. A. and D. Cortez (2008). "ATR: an essential regulator of genome integrity." Nature reviews. Molecular cell biology **9**(8): 616-627.

Clyne, R. K., V. L. Katis, et al. (2003). "Polo-like kinase Cdc5 promotes chiasmata formation and cosegregation of sister centromeres at meiosis I." Nature cell biology **5**(5): 480-485.

Crossan, G. P., L. van der Weyden, et al. (2011). "Disruption of mouse Slx4, a regulator of structure-specific nucleases, phenocopies Fanconi anemia." Nature genetics **43**(2): 147-152.

D'Andrea, A. D. (2010). "Susceptibility pathways in Fanconi's anemia and breast cancer." The New England journal of medicine **362**(20): 1909-1919.

Donaldson, M. M., A. A. Tavares, et al. (2001). "The mitotic roles of Polo-like kinase." Journal of cell science **114**(Pt 13): 2357-2358.

Evans, E., N. Sugawara, et al. (2000). "The Saccharomyces cerevisiae Msh2 mismatch repair protein localizes to recombination intermediates in vivo." Molecular cell **5**(5): 789-799.

Fanconi, G. (1967). "Familial constitutional panmyelocytopathy, Fanconi's anemia (F.A.). I. Clinical aspects." Seminars in hematology **4**(3): 233-240.

Fekairi, S., S. Scaglione, et al. (2009). "Human SLX4 is a Holliday junction resolvase subunit that binds multiple DNA repair/recombination endonucleases." Cell **138**(1): 78-89.

Fishman-Lobell, J. and J. E. Haber (1992). "Removal of nonhomologous DNA ends in double-strand break recombination: the role of the yeast ultraviolet repair gene RAD1." Science **258**(5081): 480-484.

Flott, S., C. Alabert, et al. (2007). "Phosphorylation of Slx4 by Mec1 and Tel1 regulates the single-strand annealing mode of DNA repair in budding yeast." Molecular and cellular biology **27**(18): 6433-6445.

Garaycoechea, J. I., G. P. Crossan, et al. (2012). "Genotoxic consequences of endogenous aldehydes on mouse haematopoietic stem cell function." Nature **489**(7417): 571-575.

Garcia-Higuera, I., T. Taniguchi, et al. (2001). "Interaction of the Fanconi anemia proteins and BRCA1 in a common pathway." Molecular cell **7**(2): 249-262.

Gargiulo, D., G. S. Kumar, et al. (1995). "Structural and function modification of DNA by mitomycin C. Mechanism of the DNA sequence specificity of mitomycins." Nucleic acids symposium series(34): 169-170.

Gong, L. and E. T. Yeh (1999). "Identification of the activating and conjugating enzymes of the NEDD8 conjugation pathway." The Journal of biological chemistry **274**(17): 12036-12042.

Griffith, J. D., L. Comeau, et al. (1999). "Mammalian telomeres end in a large duplex loop." Cell **97**(4): 503-514.

Grossmann, K. F., A. M. Ward, et al. (2001). "S. cerevisiae has three pathways for DNA interstrand crosslink repair." Mutation research **487**(3-4): 73-83.

Guainazzi, A., A. J. Campbell, et al. (2010). "Synthesis and molecular modeling of a nitrogen mustard DNA interstrand crosslink." Chemistry **16**(40): 12100-12103.

Gudjonsson, T., M. Altmeyer, et al. (2012). "TRIP12 and UBR5 suppress spreading of chromatin ubiquitylation at damaged chromosomes." Cell **150**(4): 697-709.

Hanada, K., M. Budzowska, et al. (2007). "The structure-specific endonuclease Mus81 contributes to replication restart by generating double-strand DNA breaks." Nature structural & molecular biology **14**(11): 1096-1104.

Hanada, K., M. Budzowska, et al. (2006). "The structure-specific endonuclease Mus81-Eme1 promotes conversion of interstrand DNA crosslinks into double-strands breaks." The EMBO journal **25**(20): 4921-4932.

Huang, H., I. D. Kozekov, et al. (2010). "DNA cross-link induced by trans-4-hydroxynonenal." **51**(6): 625-634.
Huang, J., S. Liu, et al. (2013). "The DNA translocase FANCM/MHF promotes replication traverse of DNA interstrand crosslinks." Molecular cell **52**(3): 434-446.
Ip, S. C., U. Rass, et al. (2008). "Identification of Holliday junction resolvases from humans and yeast." Nature **456**(7220): 357-361.
Iyer, R. R., A. Pluciennik, et al. (2006). "DNA mismatch repair: functions and mechanisms." Chemical reviews **106**(2): 302-323.
Jachymczyk, W. J., R. C. von Borstel, et al. (1981). "Repair of interstrand cross-links in DNA of Saccharomyces cerevisiae requires two systems for DNA repair: the RAD3 system and the RAD51 system." Molecular & general genetics : MGG **182**(2): 196-205.
Jiricny, J. (2006). "The multifaceted mismatch-repair system." Nature reviews. Molecular cell biology **7**(5): 335-346.
Kashiyama, K., Y. Nakazawa, et al. (2013). "Malfunction of nuclease ERCC1-XPF results in diverse clinical manifestations and causes Cockayne syndrome, xeroderma pigmentosum, and Fanconi anemia." American journal of human genetics **92**(5): 807-819.
Kim, S. T., D. S. Lim, et al. (1999). "Substrate specificities and identification of putative substrates of ATM kinase family members." The Journal of biological chemistry **274**(53): 37538-37543.
Kim, H. and A. D. D'Andrea (2012). "Regulation of DNA cross-link repair by the Fanconi anemia/BRCA pathway." Genes & development **26**(13): 1393-1408.
Kim, J. M., Y. Kee, et al. (2008). "Cell cycle-dependent chromatin loading of the Fanconi anemia core complex by FANCM/FAAP24." Blood **111**(10): 5215-5222.
Kim, Y., F. P. Lach, et al. (2011). "Mutations of the SLX4 gene in Fanconi anemia." Nature genetics **43**(2): 142-146.
Kim, Y., G. S. Spitz, et al. (2013). "Regulation of multiple DNA repair pathways by the Fanconi anemia protein SLX4." Blood **121**(1): 54-63.
Kirchner J.J., Sigurdsson,S.T. and Hopkins,P.B. (1992) "Interstrand cross-linking of duplex DNA by nitrous acid: covalent structure of the dG-to-dG cross-link at the sequence 5'-CG". J. Am. Chem. Soc., 114, 4021–4027.
Knipscheer, P., M. Raschle, et al. (2009). "The Fanconi anemia pathway promotes replication-dependent DNA interstrand cross-link repair." Science **326**(5960): 1698-1701.
Kratz, K., B. Schopf, et al. (2010). "Deficiency of FANCD2-associated nuclease KIAA1018/FAN1 sensitizes cells to interstrand crosslinking agents." Cell **142**(1): 77-88.
Kunkel, T. A. and D. A. Erie (2005). "DNA mismatch repair." Annual review of biochemistry **74**: 681-710.
Kuraoka, I., W. R. Kobertz, et al. (2000). "Repair of an interstrand DNA cross-link initiated by ERCC1-XPF repair/recombination nuclease." The Journal of biological chemistry **275**(34): 26632-26636.
Lawley, P. D. and D. H. Phillips (1996). "DNA adducts from chemotherapeutic agents." Mutation research **355**(1-2): 13-40.
Lee, B. H. and A. Amon (2003). "Role of Polo-like kinase CDC5 in programming meiosis I chromosome segregation." Science **300**(5618): 482-486.

Lee, J. E., M. J. Sweredoski, et al. (2011). "The steady-state repertoire of human SCF ubiquitin ligase complexes does not require ongoing Nedd8 conjugation." Molecular & cellular proteomics : MCP **10**(5): M110 006460.
Li, F., J. Dong, et al. (2008). "Microarray-based genetic screen defines SAW1, a gene required for Rad1/Rad10-dependent processing of recombination intermediates." Molecular cell **30**(3): 325-335.
Liu, L. F., S. D. Desai, et al. (2000). "Mechanism of action of camptothecin." Annals of the New York Academy of Sciences **922**: 1-10.
Liu, T., G. Ghosal, et al. (2010). "FAN1 acts with FANCI-FANCD2 to promote DNA interstrand cross-link repair." Science 329(5992): 693-696.
MacKay, C., A. C. Declais, et al. (2010). "Identification of KIAA1018/FAN1, a DNA repair nuclease recruited to DNA damage by monoubiquitinated FANCD2." Cell **142**(1): 65-76.
Matos, J., M. G. Blanco, et al. (2011). "Regulatory control of the resolution of DNA recombination intermediates during meiosis and mitosis." Cell **147**(1): 158-172.
Matsuoka, S., B. A. Ballif, et al. (2007). "ATM and ATR substrate analysis reveals extensive protein networks responsive to DNA damage." Science **316**(5828): 1160-1166.
McCabe, K. M., S. B. Olson, et al. (2009). "DNA interstrand crosslink repair in mammalian cells." Journal of cellular physiology **220**(3): 569-573.
McHugh, P. J., V. J. Spanswick, et al. (2001). "Repair of DNA interstrand crosslinks: molecular mechanisms and clinical relevance." The lancet oncology **2**(8): 483-490.
Meetei, A. R., J. P. de Winter, et al. (2003). "A novel ubiquitin ligase is deficient in Fanconi anemia." Nature genetics **35**(2): 165-170.
Mohaghegh, P. and I. D. Hickson (2001). "DNA helicase deficiencies associated with cancer predisposition and premature ageing disorders." Human molecular genetics **10**(7): 741-746.
Mu, J. J., Y. Wang, et al. (2007). "A proteomic analysis of ataxia telangiectasia-mutated (ATM)/ATM-Rad3-related (ATR) substrates identifies the ubiquitin-proteasome system as a regulator for DNA damage checkpoints." The Journal of biological chemistry **282**(24): 17330-17334.
Muniandy, P. A., D. Thapa, et al. (2009). "Repair of laser-localized DNA interstrand cross-links in G1 phase mammalian cells." The Journal of biological chemistry **284**(41): 27908-27917.
Munoz, I. M., K. Hain, et al. (2009). "Coordination of structure-specific nucleases by human SLX4/BTBD12 is required for DNA repair." Molecular cell **35**(1): 116-127.
Murnane, J. P. and J. E. Byfield (1981). "Irreparable DNA cross-links and mammalian cell lethality with bifunctional alkylating agents." Chemico-biological interactions **38**(1): 75-86.
Niedernhofer, L. J., A. S. Lalai, et al. (2005). "Fanconi anemia (cross)linked to DNA repair." Cell **123**(7): 1191-1198.
Niedernhofer, L. J., H. Odijk, et al. (2004). "The structure-specific endonuclease Ercc1-Xpf is required to resolve DNA interstrand cross-link-induced double-strand breaks." Molecular and cellular biology **24**(13): 5776-5787.
Ohh, M., W. Y. Kim, et al. (2002). "An intact NEDD8 pathway is required for Cullin-dependent ubiquitylation in mammalian cells." EMBO reports **3**(2): 177-182.
Okamoto, K., C. Bartocci, et al. (2013). "A two-step mechanism for TRF2-mediated chromosome-end protection." Nature **494**(7438): 502-505.

Palm, W. and T. de Lange (2008). "How shelterin protects mammalian telomeres." Annual review of genetics **42**: 301-334.
Pepper, C. J., R. M. Hambly, et al. (2004). "The novel sequence-specific DNA cross-linking agent SJG-136 (NSC 694501) has potent and selective in vitro cytotoxicity in human B-cell chronic lymphocytic leukemia cells with evidence of a p53-independent mechanism of cell kill." Cancer research **64**(18): 6750-6755.
Petroski, M. D. and R. J. Deshaies (2005). "Function and regulation of cullin-RING ubiquitin ligases." Nature reviews. Molecular cell biology **6**(1): 9-20.
Pickett, H. A., J. D. Henson, et al. (2011). "Normal mammalian cells negatively regulate telomere length by telomere trimming." Human molecular genetics **20**(23): 4684-4692.
Raschle, M., P. Knipscheer, et al. (2008). "Mechanism of replication-coupled DNA interstrand crosslink repair." Cell **134**(6): 969-980.
Rothfuss, A. and M. Grompe (2004). "Repair kinetics of genomic interstrand DNA cross-links: evidence for DNA double-strand break-dependent activation of the Fanconi anemia/BRCA pathway." Molecular and cellular biology **24**(1): 123-134.
Saha, A. and R. J. Deshaies (2008). "Multimodal activation of the ubiquitin ligase SCF by Nedd8 conjugation." Molecular cell **32**(1): 21-31.
Salewsky, B., M. Schmiester, et al. (2012). "The nuclease hSNM1B/Apollo is linked to the Fanconi anemia pathway via its interaction with FANCP/SLX4." Human molecular genetics **21**(22): 4948-4956.
Sharma, S. and C. E. Canman (2012). "REV1 and DNA polymerase zeta in DNA interstrand crosslink repair." Environmental and molecular mutagenesis **53**(9): 725-740.
Shay, J. W. and S. Bacchetti (1997). "A survey of telomerase activity in human cancer." European journal of cancer **33**(5): 787-791.
Singh, T. R., D. Saro, et al. (2010). "MHF1-MHF2, a histone-fold-containing protein complex, participates in the Fanconi anemia pathway via FANCM." Molecular cell **37**(6): 879-886.
Skoog, L. and G. Bjursell (1974). "Nuclear and cytoplasmic pools of deoxyribonucleoside triphosphates in Chinese hamster ovary cells." The Journal of biological chemistry **249**(20): 6434-6438.
Smogorzewska, A., R. Desetty, et al. (2010). "A genetic screen identifies FAN1, a Fanconi anemia-associated nuclease necessary for DNA interstrand crosslink repair." Molecular cell 39(1): 36-47.
Soucy, T. A., P. G. Smith, et al. (2009). "An inhibitor of NEDD8-activating enzyme as a new approach to treat cancer." Nature **458**(7239): 732-736.
Stoepker, C., K. Hain, et al. (2011). "SLX4, a coordinator of structure-specific endonucleases, is mutated in a new Fanconi anemia subtype." Nature genetics **43**(2): 138-141.
Stone, M. P., Y. J. Cho, et al. (2008). "Interstrand DNA cross-links induced by alpha,beta-unsaturated aldehydes derived from lipid peroxidation and environmental sources." Accounts of chemical research **41**(7): 793-804.
Sugawara, N., F. Paques, et al. (1997). "Role of Saccharomyces cerevisiae Msh2 and Msh3 repair proteins in double-strand break-induced recombination." Proceedings of the National Academy of Sciences of the United States of America **94**(17): 9214-9219.

Svendsen, J. M., A. Smogorzewska, et al. (2009). "Mammalian BTBD12/SLX4 assembles a Holliday junction resolvase and is required for DNA repair." Cell **138**(1): 63-77.
Taniguchi, T., I. Garcia-Higuera, et al. (2002). "S-phase-specific interaction of the Fanconi anemia protein, FANCD2, with BRCA1 and RAD51." Blood **100**(7): 2414-2420.
Tischkowitz, M. D. and S. V. Hodgson (2003). "Fanconi anaemia." Journal of medical genetics **40**(1): 1-10.
Toh, G. W., N. Sugawara, et al. (2010). "Mec1/Tel1-dependent phosphorylation of Slx4 stimulates Rad1-Rad10-dependent cleavage of non-homologous DNA tails." DNA repair **9**(6): 718-726.
Travis, L. B., E. J. Holowaty, et al. (1999). "Risk of leukemia after platinum-based chemotherapy for ovarian cancer." The New England journal of medicine **340**(5): 351-357.
Tripsianes, K., G. Folkers, et al. (2005). "The structure of the human ERCC1/XPF interaction domains reveals a complementary role for the two proteins in nucleotide excision repair." Structure **13**(12): 1849-1858.
Tucker, M. A., C. N. Coleman, et al. (1988). "Risk of second cancers after treatment for Hodgkin's disease." The New England journal of medicine **318**(2): 76-81.
Vare, D., P. Groth, et al. (2012). "DNA interstrand crosslinks induce a potent replication block followed by formation and repair of double strand breaks in intact mammalian cells." DNA repair **11**(12): 976-985.
Varshavsky, A. (2011). "The N-end rule pathway and regulation by proteolysis." Protein science : a publication of the Protein Society.
Vermeulen, K., D. R. Van Bockstaele, et al. (2003). "The cell cycle: a review of regulation, deregulation and therapeutic targets in cancer." Cell proliferation **36**(3): 131-149.
Wan, B., J. Yin, et al. (2013). "SLX4 assembles a telomere maintenance toolkit by bridging multiple endonucleases with telomeres." Cell reports **4**(5): 861-869.
Wang, A. T., B. Sengerova, et al. (2011). "Human SNM1A and XPF-ERCC1 collaborate to initiate DNA interstrand cross-link repair." Genes & development **25**(17): 1859-1870.
Wang, X., C. A. Peterson, et al. (2001). "Involvement of nucleotide excision repair in a recombination-independent and error-prone pathway of DNA interstrand cross-link repair." Molecular and cellular biology **21**(3): 713-720.
Wilson, J. S., A. M. Tejera, et al. (2013). "Localization-dependent and -independent roles of SLX4 in regulating telomeres." Cell reports **4**(5): 853-860.
Wu, K., A. Chen, et al. (2000). "Conjugation of Nedd8 to CUL1 enhances the ability of the ROC1-CUL1 complex to promote ubiquitin polymerization." The Journal of biological chemistry 275(41): 32317-32324.
Wu, L. and I. D. Hickson (2003). "The Bloom's syndrome helicase suppresses crossing over during homologous recombination." Nature **426**(6968): 870-874.
Wu, L. and I. D. Hickson (2006). "DNA helicases required for homologous recombination and repair of damaged replication forks." Annual review of genetics 40: 279-306.
Wyatt, H. D., S. Sarbajna, et al. (2013). "Coordinated actions of SLX1-SLX4 and MUS81-EME1 for Holliday junction resolution in human cells." Molecular cell **52**(2): 234-247.
Yamamoto, K. N., S. Kobayashi, et al. (2011). "Involvement of SLX4 in interstrand cross-link repair is regulated by the Fanconi anemia pathway." Proceedings of the

National Academy of Sciences of the United States of America **108**(16): 6492-6496.

Yan, Z., M. Delannoy, et al. (2010). "A histone-fold complex and FANCM form a conserved DNA-remodeling complex to maintain genome stability." Molecular cell **37**(6): 865-878.

Yan, Z., R. Guo, et al. (2012). "A ubiquitin-binding protein, FAAP20, links RNF8-mediated ubiquitination to the Fanconi anemia DNA repair network." Molecular cell **47**(1): 61-75.

Zhao, Y., X. Xiong, et al. (2012). "Targeting Cullin-RING ligases by MLN4924 induces autophagy via modulating the HIF1-REDD1-TSC1-mTORC1-DEPTOR axis." Cell death & disease **3**: e386.